Environmental Research 268 (2025) 120749

Contents lists available at ScienceDirect

Environmental Research

journal homepage: www.elsevier.com/locate/envres

Synergistic production of nitrogen-rich hydrochar and solid biofuels via co-hydrothermal carbonization of microalgae and macroalgae: When nitrogen circularity matters

Yingdong Zhou [a,**], Haiting Xiao [a], Qing Liu [a], Lan Wang [a], Yuan Gong [a], Javier Remón [b,*]

[a] College of Materials and Chemistry & Chemical Engineering, Chengdu University of Technology, Chengdu, 610059, PR China
[b] Thermochemical Processes Group, Aragón Institute for Engineering Research (I3A), University of Zaragoza, C/Mariano Esquillor s/n, 50.018, Zaragoza, Spain

ARTICLE INFO

Keywords:
Microalgae
Macroalgae
Co-hydrothermal carbonization
Nitrogen evolution
Synergies

ABSTRACT

This work explores the synergies between N-rich (*Chlorella pyrenoidosa*) microalgae and N-deficient (*Undaria pinnatifida*) macroalgae for the production of N-containing hydrochar and solid biofuels via co-hydrothermal carbonization (co-HTC). The impact of the feedstock (each alga alone and all possible binary mixtures) was comprehensively assessed under different temperatures (180–260 °C) and times (60–240 min). The synergies between micro and macroalgae governed product distribution, nitrogen transformation pathways, and hydrochar quality, with these effects varying by processing conditions. Biomass synergies enhanced hydrochar quality at lower temperatures through deoxygenation reactions and/or liquid-phase repolymerization. In contrast, at higher temperatures, interactions between carbohydrates and proteins via solid-phase Maillard and Mannich reactions decreased hydrochar fuel quality but enriched nitrogen functionalities, such as pyridine-N. Optimization revealed that high N retention and hydrochar yield (up to 23%) were achieved by mixing up to 50 wt% macroalgae with microalgae at 223 °C for 174 min, maintaining functional N content (6 wt% N, 16% pyridine-N). Additionally, an energy-dense hydrochar (34% yield and 26 MJ/kg HHV) was synergistically produced by co-treating 70 wt% microalgae and 30 wt% macroalgae at 180 °C for 60 min. This synergistic algal approach highlights the potential of synergistic algal co-HTC to enhance nitrogen circularity, improve feedstock flexibility, and support sustainable biofuel and material production from marine resources.

1. Introduction

Switching energy and chemical commodities from fossil resources to renewable biomass feedstocks is significant in relieving the energy and environmental crises and achieving carbon neutrality (Huang and Yuan, 2015). Among various biomasses, algal biomass stands out as a promising feedstock for biorefineries due to its high photosynthetic rate and CO_2 capture capacity, short growth cycle, and no competition to farmland (Ayub et al., 2022; Saravanan et al., 2023). Algae are categorized into microalgae and macroalgae depending on their cellular structure. Specifically, microalgae are unicellular microorganisms containing high proportions of lipids (20–50 wt%) and proteins (50–70 wt%) but low amounts of carbohydrates (15–50 wt%). In contrast, macroalgae are multicellular organisms with carbohydrates in a high amount (25–60 wt%), and proteins (3–40 wt%) and lipids (<5 wt%) in lower proportions (Zhou et al., 2022a). Unlike lignocellulosic plants, algae, especially microalgae, can fix inorganic nitrogen in wastewater and transform it into proteins (Coale et al., 2024). As such, developing algal biorefineries that effectively utilize this nitrogen source not only provides fuel, chemicals, and materials sustainably but also promotes nitrogen circularity and mitigates water pollution.

Hydrothermal carbonization (HTC) is a sustainable process for converting wet biomass into hydrochar under moderate conditions (180–250 °C, 2–10 MPa) (Coale et al., 2024; Shen, 2020). Hydrochar, a carbonaceous solid with improved energy density, serves as a solid biofuel with a higher heating value (HHV) of ca. 30 MJ/kg (Remón et al., 2021; Venna et al., 2021; Zhou et al., 2023b). As for microalgal biomass, the high fraction of proteins (as high as 70 wt%) makes the N content in

This article is part of a special issue entitled: WWEM-GEET-GC-2024 published in Environmental Research.

* Corresponding author.
** Corresponding author.
E-mail addresses: yingdongzhou@cdut.edu.cn (Y. Zhou), jrn@unizar.es (J. Remón).

https://doi.org/10.1016/j.envres.2024.120749
Received 14 October 2024; Received in revised form 23 December 2024; Accepted 31 December 2024
Available online 4 January 2025

the feedstock up to ca. 10 wt% (especially for microalgae) (Chen et al., 2017), which is much higher than coal, lignocellulosic biomass, and sewage sludge. During HTC, denitrogenation transforms N into organic forms in biocrude and inorganic species (NH_4^+, NO_3^-) in the aqueous phase, decreasing the N content in hydrochar to ca. 2–4 wt% (Leng et al., 2021; Zhou et al., 2022b). However, the combustion of this nitrogen fraction in hydrochar emits higher levels of harmful NO_x pollutants than other solid fuels (e.g., coal, lignite, lignocellulosic hydrochar) (Shen et al., 2018; Wang et al., 2022b). On the bright side, nitrogenous species in hydrochar, such as pyridinic and pyrrolic N, enhance their performance in applications as catalysts, adsorbents, and electrode materials (Matsagar et al., 2021; Takeyasu et al., 2021; Tian et al., 2020). Besides, the HTC of microalgae, with abundant volatile matter, also produces liquid products (biocrude and aqueous products) containing organic nitrogenous species, such as amides, nitriles, and N-heterocycles (Leng et al., 2023; Liu et al., 2021). These organic N-containing compounds can synthesize pharmaceuticals, lubricants, agrochemicals, and fabric softeners (Chandrashekhar et al., 2022; Hahn et al., 2018). Therefore, understanding nitrogen evolution mechanisms during algae HTC is paramount to optimizing product quality. It enables decreasing the N content in hydrochars for cleaner solid biofuels, tailoring N species for carbonaceous materials applications, and increasing the selectivity of organic N-containing chemicals in the liquid phases for chemical production.

Driven by the importance of N transformation and distribution within the main HTC reaction products, some publications have reported the N behavior during the thermochemical conversion of microalgae. For example, Chen et al. studied the nitrogen evolution mechanisms during algae pyrolysis (Chen et al., 2017). They found that the protein-N in the algal feedstock was transformed into pyridinic-, pyrrolic-, and quaternary-N in the biochar. Additionally, ammonia decomposed from amino acids reacted with fatty acids to form amides, which subsequently dehydrated to nitriles. Similarly, Xiao et al. reported the evolution of nitrogen during the HTC of *Spirulina* (Xiao et al., 2019). The results showed that increased processing temperature enhanced the polymerization reactions of pyrrolic-N and pyridinic-N. The study highlighted that the processing temperature was the most influential factor affecting the transformation of protein-N in microalgae into other N species during thermochemical conversion.

However, the HTC of microalgae alone produces hydrochar with low yields (20–70%) due to the highly volatile components in microalgae (Lee et al., 2018; Supraja et al., 2023; Zhou et al., 2022b). Besides, existing HTC processes face significant challenges in managing nitrogen transformation pathways and achieving high-quality carbon products. These limitations restrict their application for nitrogen-rich biomass, where nitrogen retention and by-product management are critical. Co-hydrothermal carbonization (co-HTC) of microalgae with a less reactive feedstock containing lower N content offers a promising solution to these challenges. The synergies between different feedstock components have been shown to improve hydrochar yield and quality, meeting specific performance requirements (Piccini et al., 2019; Sahoo et al., 2021; Wang et al., 2022a; Zhou et al., 2024). In this regard, Li et al. found that proteins contributed to hydrochar formation only in the presence of carbohydrates (Li et al., 2019). This effect was attributed to Maillard reactions, which enriched the proportions of N-containing functional groups on the hydrochar surface. In another study, Shen et al. investigated the structural and nitrogen evolution of hydrochar during the co-hydrothermal treatment of *Chlorella* and cornstalk (Shen et al., 2024). The results showed synergistic effects between both feedstocks, concentrating nitrogen into the hydrochar as N-containing aromatic heterocycles.

Microalgae and macroalgae are promising feedstocks for HTC due to their abundance, rapid growth, and complementary chemical compositions. Microalgae are nitrogen-rich, while macroalgae are rich in carbohydrates, offering an opportunity for synergy when co-processed (Ramachandra and Hebbale, 2020). The co-HTC process of macroalgae and microalgae can potentially increase hydrochar yields and optimize the distributions of N species in the resulting products. In addition, co-valorizing microalgae and macroalgae offers a flexible and seasonal-free approach to biomass conversion. This flexibility arises from the feedstock-dependent nature of HTC, algae biodiversity, and seasonal variations in biomass availability (Benavente et al., 2024; Hu et al., 2023). Therefore, understanding the synergies between microalgae and macroalgae during co-HTC, particularly the nitrogen transformation pathway and related mechanisms, is crucial. This knowledge will facilitate the development of innovative and sustainable algal biorefineries.

Hydrothermal carbonization (HTC) struggles with low nitrogen retention, significant nitrogen loss, and limited control over nitrogen species, restricting its use with nitrogen-rich biomass like microalgae. Therefore, this study investigates the co-HTC of *Chlorella pyrenoidosa* (microalgae) and *Undaria pinnatifida* (macroalgae) to address these limitations. The synergy between protein-rich microalgae and carbohydrate-rich macroalgae enhances hydrochar yield, nitrogen stabilization, and product quality. Key objectives include: (1) evaluating feedstock composition effects on hydrochar yield, quality, and nitrogen circularity and (2) optimizing co-HTC to produce high-value hydrochar with tailored properties. This work demonstrates the potential of co-HTC to enable flexible, sustainable algal biorefineries for efficient fuel and chemical production.

2. Experimental section

2.1. Materials

The microalgae (*Chlorella pyrenoidosa*, CP) and macroalgae (*Undaria pinnatifida*, UP) were commercially purchased as a dry powder and used without additional treatment. All chemicals used in this study were sourced from Greagent Chemical Company without further purification. The elemental, biochemical, and proximate analyses of the feedstocks are summarized in Table 1. The results show that microalgae contain less ash than macroalgae. Regarding biochemical composition,

Table 1
Characterization results of CP and UP.

Characterization	Microalgae	Macroalgae	Test methods
Proximate (wt%)			
Moisture	5.1	6.5	Thermogravimetric analysis (GB/
Ash	4.7	12.6	T28731-2012)
Elemental (wt%)			
C	47.0	38.5	Characterized using Elementar
H	6.9	5.7	Vario EL cube
N	8.0	2.3	
O[a]	28.1	27.9	O (wt%) = 100 − C − H − N − Ash
HHV[b]	19.8	15.8	Calculated according to Friedl et al. (Friedl et al., 2005)
Biochemical (wt%)			
Lipids	15.6	10.6	Soxhlet extraction method (Manirakiza et al., 2001)
Carbohydrates	21.9	41.3	DNS colorimetric analysis (Deng and Tabatabai, 1994)
Proteins	50.2	14.3	N element content (wt%) × 6.25 (Boisen et al., 1987)
Others[c]	2.5	14.7	Calculated by deference
N-containing species (%)			
Protein-N	86.6	85.1	Characterized by XPS
Pyridine-N	4.7	3.6	
Pyrrole-N	4.7	6.3	
Quaternary-N	3.9	5.0	

[a] Organic O.
[b] HHV (MJ/kg) = $(3.55 \times C^2 - 232 \times C - 2230 \times H + 51.2 \times C \times H + 131 \times N + 20600) \times 10^{-3}$.
[c] Others include ash, pigments, and volatile organic compounds in the feedstocks.

microalgae have higher amounts of lipids and proteins and a lower proportion of carbohydrates compared to macroalgae. In addition, N in the feedstocks exists primarily as protein, pyridinic, pyrrolic, and quaternary N. Protein-N is the dominant form (>85 wt%) in both feedstocks, whereas the proportions of other forms of nitrogen are lower than 7 wt %.

2.2. Co-hydrothermal carbonization experiments

The co-HTC experiments were carried out in a 100 mL Hastelloy-lined autoclave equipped with a speed-controlled mechanic stirrer. In each experiment, 4 g of algae (i.e., CP, UP, or their binary mixture) and 40 g of deionized water were added to the reactor. The reactor was pressurized with 2 MPa of N_2 at room temperature (~25 °C) to purge air before starting the reaction. During the reaction, the pressure varied depending on the reaction temperature. The initial and final pressure ranges at reaction conditions were 3.0–3.5 MPa at 180 °C, 4.0–5.0 MPa at 220 °C, and 6.5–7.5 MPa at 260 °C. These pressure variations result from the thermal expansion of the reaction mixture and the generation of gaseous products under different temperature conditions. The autoclave was heated to the designated reaction temperature, marking the start of the processing time, with a stirring rate at 400 rpm. After the reaction, the autoclave was rapidly cooled in cold water to approximately 30 °C, depressurized, and opened. The reaction mixture containing the solid and aqueous fractions was collected. The inner wall and stirrer bar were rinsed twice with ethyl acetate to recover any remaining products. The liquid products (organic and aqueous phases) and solid hydrochar were separated via vacuum filtration. Finally, the organic phase was processed using rotary evaporation to remove the solvent, yielding biocrude. The hydrochar and biocrude were then weighed and stored for subsequent characterization.

2.3. Product characterization and response variables

The yields of co-HTC products (hydrochar, biocrude and aqueous + gas) and their key nitrogen-related properties were used as the response variables to assess the impacts of the algae mixture composition (microalgae and macroalgae), temperature (180–260 °C), and time (60–240 min) on the co-HTC process. These response variables and their corresponding calculation/characterization methods are listed in Table 2. Briefly, the elemental compositions of the hydrochar and biocrude were analyzed using an elemental analyzer (Elementar Vario EL cube). The HHV of the hydrochar and biocrude was estimated using the Friedl formula (Friedl et al., 2005), which has been extensively validated and widely applied in recent studies for predicting the HHV of biomass feedstocks and their conversion products, including hydrothermal carbonization (HTC) products (Hassan et al., 2024; Jana et al., 2025; Kostyniuk and Likozar, 2024; Zhu et al., 2024). The N species on the hydrochar surface were characterized by X-ray photoelectron spectroscopy (XPS) using a Shimadzu/Krayos AXIS Ultra DLD spectrometer equipped with Al-Kα radiation. The carbon 1s binding energy was adjusted to 284.6 eV for surface-charging corrections. The chemical composition of the biocrude was determined using a Shimadzu GCMS-QP2010 SE gas chromatography-mass spectrometer (GC-MS) with an SK-5MS column. Prior to analysis, the biocrude sample was dissolved in ethyl acetate. Total nitrogen in the aqueous phase was measured with a Jena Multi N/C 3100 Total Organic Carbon/Total Nitrogen Analyzer. NH_4^+ and NO_3^- nitrogen were quantified using the salicylate–hypochlorite method (Bower and Holm-Hansen, 1980) and salicylic acid nitration method (Cataldo et al., 1975), respectively.

2.4. Experimental model and statistical analysis methodologies

The co-HTC experiments were designed following a two-level, three-factor (2^3) Box-Wilson Central Composite Face Centered (CCF, α: ±1) method. This approach evaluates the impact of the algae feedstock composition (microalgae/(microalgae + macroalgae), 0–100 wt%), hydrothermal carbonization temperatures (180–260 °C), and times (60–240 min). This design was composed of 8 factorial experiments to analyze the linear effects and first-order interactions (Run 1–8), 6 axial experiments to determine quadratic effects and non-linear interactions (Run 9–14), and 4 center-point repeated experiments to evaluate the experimental error and variance (Run 15–18).

The experimental data were analyzed using ANOVA at a 95% confidence level (p-value ≤0.05) to evaluate the factor significance. A cause-effect Pareto test compared the relative importance of the co-HTC parameters. Factor limits (feedstock composition, temperature, and time) were normalized between −1 and + 1 to enable direct comparison. Interaction plots were developed based on the ANOVA-derived formulae of all 18 experimental runs to visually illustrate the effects of processing variables and their interactions on the co-HTC process. These plots included experimental data points to validate the lack of fit as statistically insignificant. The Least Significant Difference (LSD) bars, derived from ANOVA, were incorporated into the plots to represent pairwise

Table 2
Response variables and methods.

Product	Response variable	Method
Hydrochar	$Hydrochar\ yield\ (\%) = \frac{mass\ of\ hydrochar\ (g)}{mass\ of\ total\ biomass\ (g)} \times 100\%$	Gravimetric
	$C,H,O,N\ (\%) = \frac{mass\ of\ C,H,O,N\ (g)}{mass\ of hydrochar\ (g)} \times 100\%$	Elemental analysis (C, H, N); O (%) = 100 − C − H – N, including contributions from both organic oxygen and ash
	HHV (MJ/kg) = (3.55 × C^2 -232 × C – 2230 × H + 51.2 × C × H + 131 × N +20600) × 10^{-3}	Estimated according to Friedl et al. (Friedl et al., 2005)
	$N\ species\ on\ the\ hydrochar\ (\%) = \frac{area\ of\ each\ species}{total\ area} \times 100\%$	XPS
Biocrude	$Biocrude\ yield\ (\%) = \frac{mass\ of\ biocrude\ (g)}{mass\ of\ total\ biomass\ (g)} \times 100\%$	Gravimetric
	$C,H,O,N\ (\%) = \frac{mass\ of\ C,H,O,N\ (g)}{mass\ of biocrude\ (g)} \times 100\%$	Elemental analysis (C, H, N); O (%) = 100 − C − H − N, including contributions from both organic oxygen and ash
	HHV (MJ/kg) = (3.55 × C^2 -232 × C – 2230 × H + 51.2 × C × H + 131 × N +20600) × 10^{-3}	Estimated according to Friedl et al. (Friedl et al., 2005)
	$Composition\ (area,\%) = \frac{area\ of\ each\ compound}{total\ area} \times 100\%$	GC-MS
Aqueous and gas	$Aqueous + gas\ yield\ (\%) = 100\% - (biocrude\ yield + hydrochar\ yield)$	Balance
	Total nitrogen (mg/L)	Characterized using Jena Multi N/C 3100 Analyzer
	NH_4^+ N (mg/L)	Analyzed by colorimetry methods (Bower and Holm-Hansen, 1980; Cataldo et al., 1975)
	NO_3^- N (mg/L)	
	Organic nitrogen (mg/L) = total N − NH_4^+ N − NO_3^- N	Balance
Energy efficiency	$E(\%) = \frac{biocrude\ yield \times HHV + hydrochar\ yield \times HHV}{micro\ algae \cdot micro\ algae\ HHV + macro\ algae \cdot macro\ algae\ HHV}$	Calculated

comparisons between data points within each plot. Overlapping LSD bars indicate no statistically significant difference, while non-overlapping bars signify statistical significance at the 95% confidence level. Unlike conventional error bars, which typically reflect variability or confidence intervals, the LSD intervals specifically highlight statistical significance in the context of the experimental design. These bars also account for experimental errors, system variance, confidence intervals, and unexplained variation, providing a robust statistical framework for interpreting the results.

3. Results and discussion

Table 3 provides the algal feedstock composition (microalgae/total algae), co-HTC parameters (temperature and time), and the resulting product yields (hydrochar, biocrude, and aqueous + gas). It also includes the essential characteristics of hydrochar (elemental and surface N-containing species compositions), biocrude (elemental and chemical composition), and aqueous products (the amounts of N-containing species). The results of the ANOVA and Pareto tests, which analyze the full effects of processing parameters on the product yields and properties, are listed in Table S1.

3.1. Product yields: hydrochar, biocrude, aqueous phase + gas

The co-HTC of CP (microalgae) and UP (macroalgae) produces hydrochar (12–35%), biocrude (7–28%), and aqueous and gaseous products (56–70%). The cause-effect Pareto test shows that the hydrochar and biocrude yields are significantly affected by the reaction temperature (>29%) and feedstock composition (9%), whereas the residence time is the most influential factor for the aqueous + gas yield (13%). The quadratic terms of feedstock (F^2) are statistically significant for all product yields, indicating that the synergies between CP and UP direct the overall distribution of products. The ratio of all quadratic terms to the total feedstock effects, $F^2/(F + F^2)$, further quantifies these synergies. These data reveal notable synergies between feedstocks (33% for hydrochar yield, 35% for biocrude yield, and 54% for aqueous + gas yields). In addition, the interactions between feedstock, temperature, and time significantly impact the product yields. To illustrate these effects, Fig. 1 A/D/G, B/E/H, and C/F/I show the influence of feedstock composition at two temperatures (180 and 260 °C) across three-time intervals: short (60 min), medium (150 min), and long (240 min), respectively.

3.1.1. Influence of the alga feedstock mixture

The impact of the algae feedstock mixture varies with the reaction temperature and time. At a low temperature (180 °C), the feedstock composition exerts a similar influence regardless of the reaction time. Notably, the hydrochar yield increases progressively at the expense of the biocrude, aqueous and gaseous products by augmenting the proportion of microalgae in the feedstock. This could be accounted for by the distinct characteristics of the two algae: the microalgae are hydrophobic and lipid-rich, whereas the macroalgae are hydrophilic and carbohydrate-rich. Under hydrothermal conditions at low temperatures, the hydrolysis and dehydration of carbohydrates, which dominate macroalgae, are more likely to occur (Gomes-Dias et al., 2020). Consequently, macroalgae produce slightly higher biocrude yields than microalgae in these conditions. Besides, the variation of product yields follows a non-linear pattern, indicating interactions between the two kinds of algae ruling the product distribution. Notably, the yields to hydrochar and gas + aqueous follow a convex pattern, denoting synergies, while the biocrude yield follows a concave trend due to an antagonistic effect. As a result, the yields to hydrochar and gas + liquid obtained with a mixture comprising micro and macroalgae surpass the theoretical yields based on the individual contribution of each feedstock. In comparison, the biocrude yield from the mixture is lower than the predicted yield based on the individual algae contributions.

The processing temperature significantly influences the effect of feedstock composition on the product distribution during co-HTC. Increasing the temperature from 180 to 260 °C alters the impacts of feedstock composition, with these effects varying depending on the reaction time. At a short residence time (60 min), feedstock composition has minimal influence on the hydrochar yield but boosts the biocrude yield as the microalgae proportion rises. This could be ascribed to the abundant lipids and proteins in microalgae, readily transformed into hydrophobic biocrude at a high temperature. This observation aligns with a recent publication about co-hydrothermal liquefaction of microalgae and macroalgae (Wang et al., 2022a). Simultaneously, the aqueous + gas yield decreases convexly, reaching a maximum with a feedstock comprising c.a. 40/60 wt% micro/macroalgae. In addition, prolonging the reaction time from 60 to 240 min intensifies the synergistic effect on the formation of hydrochar and gaseous + liquid products and enhances the antagonistic effects on biocrude formation. These trends make the yield curves more convex for hydrochar and gaseous + liquid products (Fig. 1 A, B, C, G, H, I) and more concave for biocrude (Fig. 1 D, E, F). These variations are possibly attributed to the positive kinetic effect of the solid-phase Maillard/Mannich reaction between carbohydrates and proteins and the repolymerization of N-containing species in biocrude into the N-heterocyclic polymers. These chemical transformations are more prominent at higher temperatures and longer reaction times during the co-HTC of micro- and macroalgae (Li et al., 2019; Xiao et al., 2019).

3.1.2. Influence of the co-HTC temperature and time

The co-HTC temperature affects the overall distribution of products significantly. Regardless of the feedstock, increasing the temperature from 180 to 260 °C augments the biocrude yield while decreasing the hydrochar yield. However, this temperature effect is more pronounced in microalgae-rich feedstocks due to the higher contribution of lipids and proteins, which are abundant in microalgae, to biocrude formation. In contrast, carbohydrate-derived species are more likely to convert into hydrochar via dehydration, aromatization, and condensation reactions at elevated temperatures (Sevilla and Fuertes, 2009). The effect of the reaction time depends on the temperature. At 180 °C, prolonging the residence time from 60 to 240 min increases the yields of biocrude, aqueous and gaseous products at the expense of hydrochar yield, regardless of the feedstock composition. At 260 °C, such a time increment decreases the biocrude yield regardless of the feedstock composition. These outcomes result from different reactions, such as depolymerization, repolymerization, and condensation, governing algal component conversion and dissolution, with different outcomes depending on the temperature. At 180 °C, a positive kinetic effect promotes the depolymerization and dissolution of microalgae/macroalgae components into organic biocrude, aqueous inorganic species, and gaseous products. At a high temperature like 260 °C, the liquid intermediates/products tend to be repolymerized to form hydrochar by prolonging the residence time.

3.2. Hydrochar elemental composition and HHV

The elemental composition of hydrochar varies between 48 and 67 wt% for C, 5–7 wt% for H, 20–42 wt% for O, and 3–9 wt% for N, resulting in a calorific value between 20 and 29 wt%. The ANOVA and cause-effect Pareto test (Table S1) identify the feedstock composition (micro/macro alga relationship) as the most influential parameter affecting these properties. The quadratic contribution with respect to the total feedstock influence, i.e., $F^2/(F^2+F)$, reveals synergies between the algae directing the elemental composition and HHV (17% for N, 48–67% for other elements, and HHV). The effect of the feedstock mixture on the elemental composition and HHV of the hydrochar is plotted across temperatures (180–260 °C) and times (60, 150, and 240 min) in Fig. 2 A/D/G/J/M, B/E/H/K/N, and C/F/I/L/O, respectively.

Table 3
Co-HTC conditions and experimental results.

Run	1	2	3	4	5	6	7	8	9	10	11	12	13	14	15–18
Algae proportion (wt%)	0	100	0	100	0	100	0	100	0	100	50	50	50	50	50
T (°C)	180	180	260	260	180	180	260	260	220	220	180	260	220	220	220
t (min)	60	60	60	60	240	240	240	240	150	150	150	150	60	240	150
Global product distribution															
Hydrochar yield (wt %)	27.71	34.69	18.49	16.61	24.03	22.88	19.27	11.70	27.64	12.40	31.13	17.29	23.26	22.13	23.35 ± 0.43
Biocrude yield (wt %)	11.56	8.04	18.08	27.60	12.35	14.53	16.99	24.68	10.78	18.08	7.43	18.00	18.15	17.80	18.66 ± 0.44
Aqueous + gas yield (wt %)	60.73	57.27	63.43	55.79	63.62	62.59	63.74	63.62	61.58	69.52	61.44	64.71	58.59	60.07	57.99 ± 0.47
Hydrochar elemental composition and HHV															
C (wt.%)	48.11	55.93	62.77	59.56	54.45	60.21	67.46	66.68	57.98	61.03	60.21	59.91	59.56	58.63	58.18 ± 1.41
H (wt.%)	6.97	7.35	5.08	6.35	5.59	6.49	5.73	6.31	5.49	6.01	6.49	6.46	6.35	5.53	5.63 ± 0.16
O (wt.%)	41.51	28.19	28.28	24.89	36.92	24.14	23.08	19.98	33.15	24.97	27.18	28.15	28.41	30.19	30.42 ± 1.60
N (wt.%)	3.41	8.53	3.87	9.2	3.04	9.16	3.73	7.03	3.38	7.99	6.12	5.48	5.68	5.65	5.78 ± 0.06
HHV (MJ/Kg)	19.73	24.50	25.53	25.78	22.01	26.24	28.61	29.30	23.58	26.09	25.84	25.57	25.32	24.21	24.10 ± 0.78
Hydrochar surface N-species composition (area, %)															
Pyridine-N	8.11	7.55	15.90	20.11	12.87	8.16	21.25	23.49	12.86	14.36	11.88	26.34	14.20	18.63	14.60 ± 0.97
Protein-N	77.41	80.09	69.38	64.46	71.52	78.73	63.36	58.79	67.18	67.41	75.85	63.35	70.91	67.36	67.65 ± 0.66
Pyrrole-N	6.43	6.71	3.15	6.53	7.03	7.28	0.00	6.14	10.36	10.77	5.94	0.00	7.99	6.00	10.49 ± 0.84
Quaternary-N	8.05	5.65	11.56	8.91	8.58	5.83	15.39	11.58	9.60	7.46	6.33	10.31	6.89	8.01	7.27 ± 0.40
Biocrude elemental composition and HHV															
C (wt.%)	60.24	71.63	69.26	68.37	59.49	71.24	69.87	72.56	66.60	67.76	70.22	71.51	65.48	71.52	69.48 ± 0.70
H (wt.%)	6.63	9.53	7.15	8.60	6.79	9.49	7.35	8.91	7.57	9.15	9.40	8.32	8.14	8.48	8.33 ± 0.35
O (wt.%)	31.37	16.11	20.28	18.34	31.44	16.26	19.44	13.46	22.77	19.45	18.14	15.22	22.76	15.44	18.24 ± 0.85
N (wt.%)	1.96	2.72	3.31	4.70	2.28	3.01	3.34	5.07	3.06	3.64	2.24	4.96	3.62	4.56	3.95 ± 0.15
HHV (MJ/Kg)	24.83	35.40	30.76	32.09	24.59	35.07	31.40	35.55	29.54	32.17	34.10	33.96	29.51	34.14	32.44 ± 0.66
Biocrude chemical composition (area, %)															
Aliphatic compounds	77.33	91.98	68.5	75.44	70.17	96.38	50.03	67.69	69.86	90.15	89.53	73.26	87.22	78.22	83.04 ± 1.69
Phenols	8.44	3.60	14.75	3.61	2.88	1.64	28.08	1.92	7.35	0.69	2.52	3.38	3.64	3.96	2.85 ± 1.21
Other oxygenated compounds	5.42	0.30	0.61	1.18	17.30	0.36	3.35	2.00	4.30	1.12	1.44	2.87	0.19	1.81	1.44 ± 0.65
Amides	6.60	2.81	4.64	16.23	2.03	0.43	5.03	23.23	10.40	6.01	4.93	16.36	5.46	11.40	8.48 ± 2.54
N-heterocycles	2.22	1.30	10.49	3.54	7.62	1.18	13.51	5.03	8.08	2.03	1.58	4.14	3.50	4.97	4.21 ± 1.30
Aqueous N-containing species concentration (mg/L)															
Total N	596	2981	944	4357	519	3688	975	5375	952	4777	2254	2478	1969	3115	2967 ± 58
Organic N	59	2150	408	3169	73	2990	203	2895	620	3371	1710	1343	1379	1601	1713 ± 86
NO_3^--N	110.1	57.8	27.9	20.6	37.5	43.9	25.2	17.6	53.1	38.3	60.2	17.8	32.0	36.1	36.1 ± 3.5
NH_4^+-N	427	772	508	1167	408	653	747	2462	279	1367	484	1117	557	1477	1018 ± 103

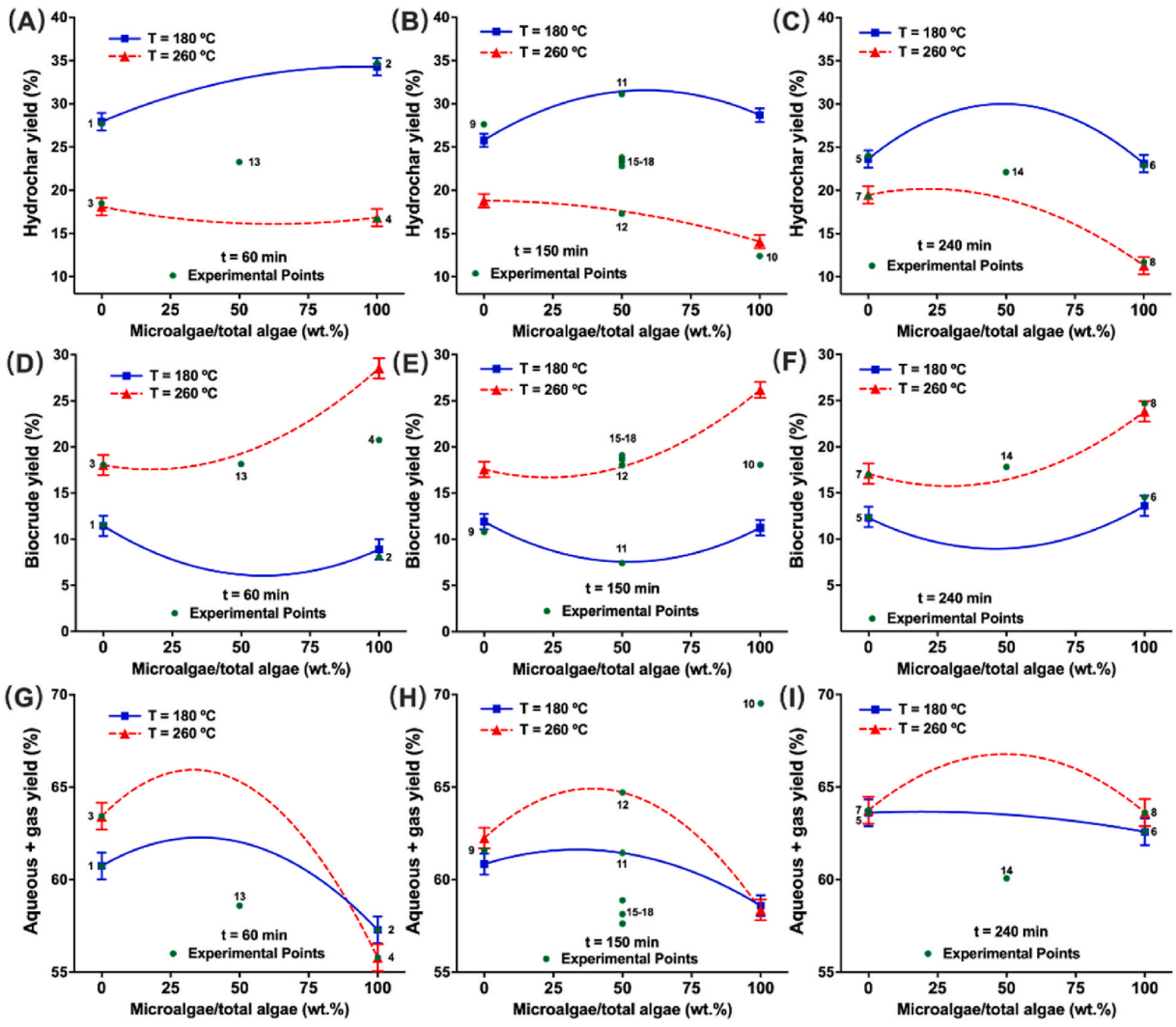

Fig. 1. The influence of feedstock mix (microalgae and macroalgae) on the overall yields of products at 180 and 260 °C for a residence time of 60, 150, and 240 min. Error bars display LSD intervals for the whole variation interval.

3.2.1. *Influence of the alga feedstock mixture*

The composition of the algal feedstock mixture significantly influences the elemental composition and HHV of the hydrochar, with effects dependent on the temperature and time. At 180 °C, the hydrochar produced from pure CP contains higher proportions of C, H, and N and a lower content of O compared to the hydrochar from pure UP. Augmenting the CP proportion in the feedstock results in a linear increment in the H and N contents and a concave diminishment in the O proportion in the hydrochar. The significant difference in elemental composition between the feedstocks causes these linear evolutions. Exceptionally, increasing the microalgae proportion in the feedstock leads to an early increase (0–65 wt% microalgae/total algae) and a successive decrease (65–100 wt%) in C. These variations jointly result in a convex development of the hydrochar HHV. These results suggest synergistic interactions between microalgal and macroalgal feedstocks, enhancing solid biofuel quality at a low temperature (180 °C). Some of these synergies may result from the dissolution of O-rich species, repolymerization of energetic species, and the deoxygenation reaction in the hydrochar. These reactions are synergistically promoted by the acidic intermediates (formic acid, acetic acids, amino acids) generated from polysaccharides and protein degradation) at low temperatures (Gu et al., 2022; Jiang et al., 2018). At 260 °C, the hydrochar derived from pure UP contains higher levels of C and O but lower proportions of H and N compared to hydrochar from pure CP. Consequently, CP-derived hydrochar achieves a slightly higher HHV than UP-derived hydrochar. Increasing the microalgae proportion in the feedstock results in a concave pattern of the C content and HHV, contrasting with the convex trends at 180 °C, while H and N contents follow a convex pattern. These results suggest an antagonistic interaction between the algae materials at a high temperature, directing the calorific value of the hydrochar. Such antagonism results from the repolymerization of O-rich species (abundant in macroalgae) and the enhanced Maillard/Mannich reactions between proteins and carbohydrate-derived species (abundant in microalgae and macroalgae) at high temperatures. As a result, hydrochar formation increases at the expense of its calorific value (Li et al., 2019).

In addition to the reaction temperature, the residence time significantly influences the synergy between feedstocks. Although qualitative trends remain similar regardless of the residence time, the quantitative influence varies. Specifically, prolonging reaction time from 60 to 240 min weakens these synergistic effects, directing the elemental composition and HHV of the hydrochar at 180 °C but strengthening the antagonistic effects at 260 °C, resulting in less or more concave/convex curves in the interaction plots, respectively.

3.2.2. *Impacts of the co-HTC temperature and time*

The effect of the temperature on the C and O contents and HHV of hydrochar depends on the feedstock mixture. For macroalgae and

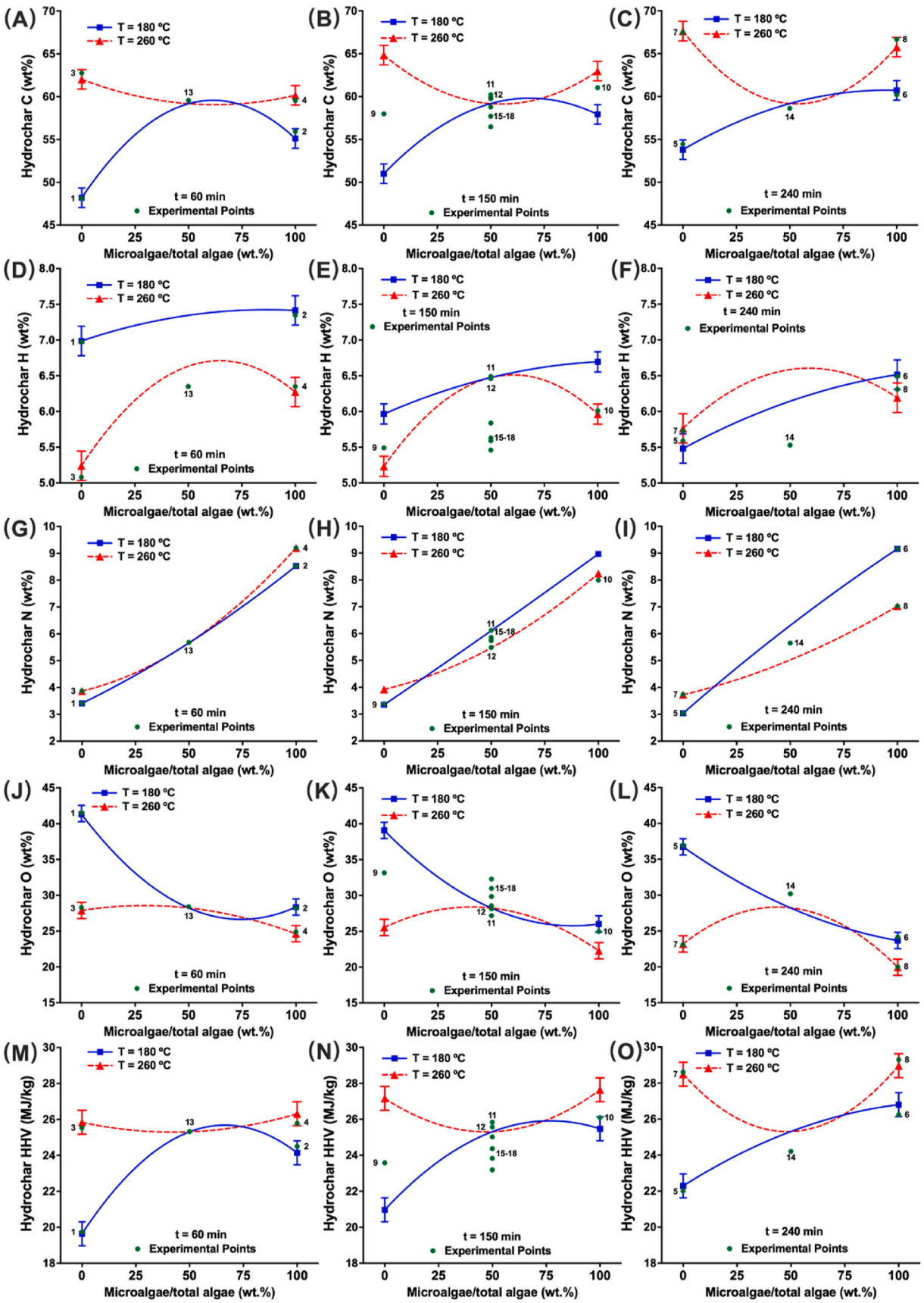

Fig. 2. The Influence of feedstock mix (microalgae and macroalgae) on the elemental composition and HHV of hydrochar at 180 and 260 °C for a residence time of 60, 150, and 240 min. Error bars display LSD intervals for the whole variation interval.

microalgae-rich mixtures, increasing the processing temperature augments the proportion of C while decreasing the contents of O and H, thereby boosting the hydrochar HHV. In contrast, switching the feedstock from macroalgae to microalgae weakens these evolutions, although the temperature effect on the H content remains independent of the feedstock. These results suggest that higher temperatures promote the deoxygenation (via dehydration, decarboxylation, and decarbonylation) of the hydrochar (Cao et al., 2021; Lin et al., 2024; Zhou et al., 2023a). The decarboxylation and decarbonylation reactions are more pronounced during the HTC of macroalgae than microalgae. As an exception, augmenting the temperature has little impact on the N content in the hydrochar. Similarly, the influence of reaction time on the hydrochar elemental composition and HHV is statistically insignificant. Irrespective of the feedstock composition or reaction temperature, extending the reaction time from 60 to 240 min increases C proportions and decreases the N and O contents, with these effects being more pronounced at lower temperatures. At higher temperatures, the positive kinetic effect masks the impact of reaction time. Exceptionally, the impact of the reaction time on the H content depends on the temperature. Extending the reaction time from 60 to 240 min decreases the H content at 180 °C and increases it marginally at 260 °C, although such changes are negligible in practical terms.

3.3. N-containing species distribution on the hydrochar

Based on the elemental analysis, the nitrogen content in hydrochar shows significant variation with changes in feedstock composition, indicating potential shifts in hydrochar formation pathways and the evolution of N-containing species on the hydrochar surface. To investigate this, the distribution of surface N species has been analyzed using XPS, as depicted in Fig. S1. The N 1s peak is deconvoluted into four distinct components, identified as pyridine-N (398.2 ± 0.2 eV), protein-N (399.8 ± 0.2 eV), pyrrole-N (400.6 ± 0.1 eV), and quaternary-N (401.3 ± 0.1 eV), based on previous studies (Shen et al., 2024; Wang et al., 2018, 2022b; Xiao et al., 2019). Their relative abundance is quantified by normalizing the peak areas, showing that the hydrochar surface contains pyridine-N (8–26%), protein-N (59–80%), pyrrole-N (0–12%), and quaternary-N (6–15%). Protein-N, initially present as proteins in algae, transforms pyrrolic, pyridinic, and quaternary-N during the co-HTC process. The ANOVA and Pareto test (Table S1) show that the composition of the algae mixture and co-HTC temperature significantly influence the distribution of the surface N-species. The synergistic and antagonist effects between algae feedstocks are quantified by the quadratic terms relative to the total feedstock effects, i.e., $F^2/(F + F^2)$. These synergistic effects account for 44–56% of pyridinic, pyrrolic, and quaternary forms of nitrogen, while protein-N shows negligible synergistic influences. In addition, the triple interactions (feedstock-temperature-time, FTt) are statistically insignificant. A representative example, the impact of feedstock composition on N-species distribution, is plotted at 180 and 260 °C for 150 min in Fig. 3, with the same evolutions taking place at the temperature range studied.

3.3.1. Influence of the algae feedstock mixture

The impact of the feedstock composition on the proportions of pyridinic, protein, and pyrrolic N on the hydrochar varies with the co-HTC temperature. At 180 °C, the hydrochar derived from pure UP and CP contains similar amounts of pyridinic and pyrrolic N. Conversely, the hydrochar from macroalgae contains more quaternary-N and less

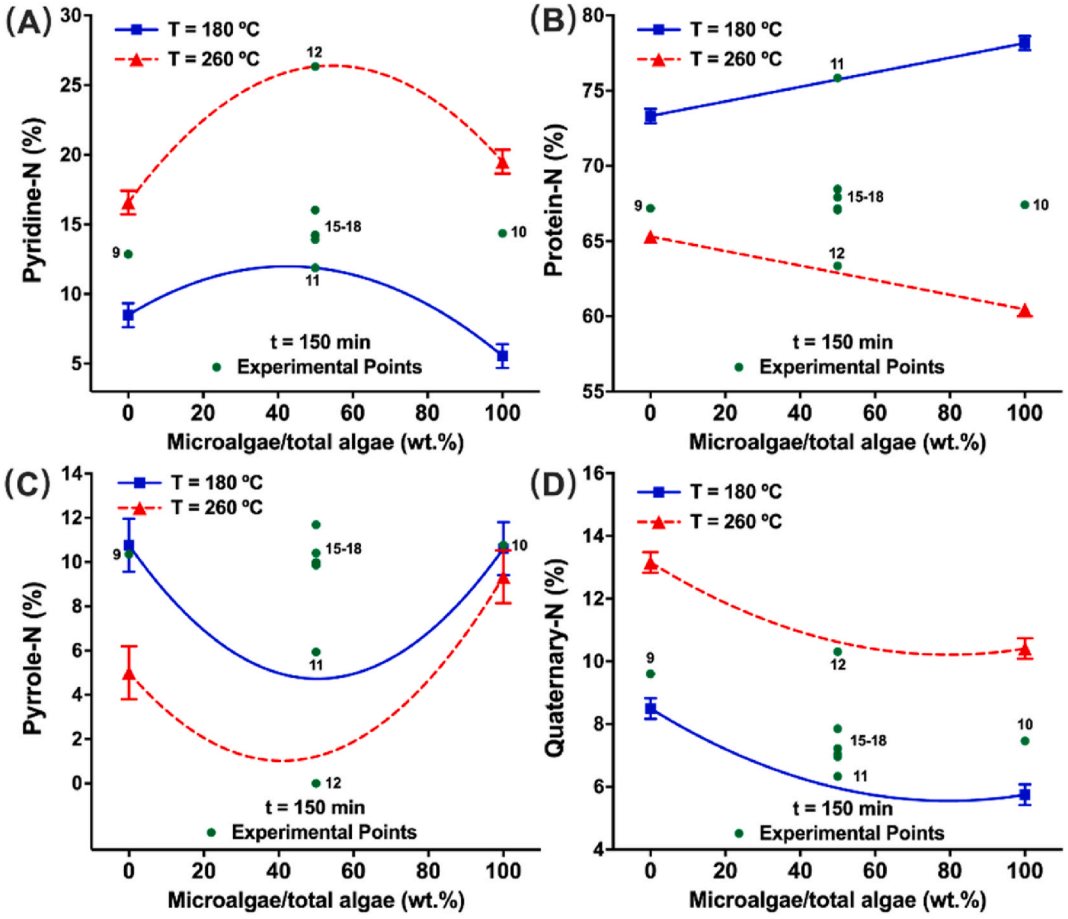

Fig. 3. The influence of feedstock mix (microalgae and macroalgae) on the N-containing species on the hydrochar at 180 and 260 °C for 150 min. Error bars display LSD intervals for the whole variation interval.

protein-N compared to the hydrochar from pure microalgae. However, strong synergies between macro- and microalgae impact the proportions of pyridinic and pyrrolic nitrogen on the hydrochar. Specifically, increasing CP proportion in the feedstock initially increases pyridinic nitrogen content, peaking with an equimassic CP and UP mixture, followed by a decline. Contrarily, switching the feedstock from UP gradually to CP results in a concave evolution of the pyrrolic nitrogen. These evolutions indicate synergistic and antagonist effects between algae feedstocks pyridine-N and pyrrole-N, respectively. This could be ascribed to the intensified Maillard reactions, where carbohydrate-rich macroalgae and protein-rich microalgae interact in the same medium to form more pyridine-N and pyrrole-N (Shen et al., 2024; Wang et al., 2018). Aldehydes derived from the carbohydrates react with pyrrole-N via Mannich reactions to form more stable pyridine-N (Shen et al., 2024), thus driving the synergistic effect on pyridine-N and antagonist effect on pyrrole-N. In comparison, the synergies between materials are less crucial for protein-N proportions. Switching the feedstock from UP to CP increases the protein-N content linearly at 180 °C due to the higher amount of protein-N in CP. However, raising CP content in the feedstock diminishes quaternary-N content concavely, regardless of the processing temperature.

At 260 °C, the hydrochar produced from pure UP contains higher contents of protein-N and lower proportions of pyrrole-N and pyridine-N than those from CP. Thus, adding more CP into the feedstock leads to a convex increment in pyridine-N content and a concave increment in pyrrole-N content. These evolutions indicate synergies between algae feedstocks, similar to the phenomena at 200 °C. In contrast, the variation in the protein-N content follows a linear pattern, decreasing with higher CP proportions. Such developments could result from converting the protein-N, which is more abundant in microalgae, into pyridine and pyrrole-N with high preference at a high temperature.

3.3.2. Impact of the co-HTC temperature

The impact of the processing temperature varies with the feedstock mixture. Augmenting the co-HTC temperature from 180 to 260 °C increases pyridinic and quaternary N proportions while reducing pyrrolic and protein-N contents. These variations are more pronounced with a higher proportion of the microalgae in the feedstock mixture, particularly for pyridinic and protein-N, whereas pyrrolic-N changes are less significant. This suggests that protein-N and pyrrole-N are more likely to be transformed into pyridine-N and quaternary-N, which are more stable, via Maillard, Mannich, condensation, and cyclization reactions (Shen et al., 2024; Wang et al., 2018; Xiao et al., 2019). Such reactions are more favored in microalgae due to their higher protein content compared to macroalgae.

3.4. Biocrude elemental composition and HHV

The elemental composition of biocrude ranges from 59 to 73 wt% C, 7–10 wt% H, 2–5 wt% N, and 13–31 wt% O, with its HHV turning between 20 and 29 MJ/kg. The ANOVA and Pareto test suggest that the feedstock composition (including linear and quadratic influences) significantly affects the biocrude elemental composition and HHV. The ratio of $F^2/(F+F^2)$ exceeds 27% for the C, N, O contents, and HHV of the biocrude, indicating significant synergies between microalgae and macroalgae that substantially affect the calorific properties of the biocrude. Fig. 4A–C/D-F/G-I/J-L/M-O illustrates these effects on the proportions of C/H/N/O and the HHV of biocrude at 180 and 260 °C for 60, 150, and 240 min.

3.4.1. Influence of the algae feedstock mixture

The impact of the algal feedstock mixture on biocrude properties depends on the processing temperature and time. At a low temperature (180 °C), the biocrude from pure CP contains higher C, H, and N contents and a lower proportion of O, resulting in a higher HHV than macroalgal biocrude, irrespective of the reaction time. This is attributed to more lipids in CP, which provides more C and H atoms, and its protein content, which contributes to N, which is prone to dissolving and liquefying at a low temperature. Augmenting the proportion of UP in the feedstock mixture enhances the relative contents of C, H, and N and decreases the amount of O. The changes in H, O, and HHV follow a linear pattern, whereas the increments in C and N are non-linear. This indicates both synergistic and antagonist effects directing C and N proportions during biocrude formation. At 180 °C, the biocrude primarily forms via the dissolution of algal components. Therefore, the biocrude elemental composition mainly depends on feedstock elemental composition, resulting in unmarked synergies under this co-HTC condition. At 260 °C, the impacts of the feedstock are less marked. The biocrude from UP comprises a similar amount of C, higher amounts of H and N, and a lower proportion of O compared to CP biocrude, leading to a more energetic biocrude from CP. The variations in C and N are non-linear, suggesting possible synergies between materials at higher temperatures. These might be accounted for by enhanced Maillard, Mannich, and amidation reactions at a high temperature, promoting the liquefaction of N-containing species of the feedstocks and hydrochar. These observations align with the literature (Shen et al., 2024; Xiao et al., 2019).

In addition, prolonging the reaction time intensifies the synergies between microalgae and macroalgae, improving biocrude quality regardless of the processing temperature. These effects are more marked at lower temperatures compared to higher ones. This is evidenced by the non-linear changes in C, H, and O contents and HHV of biocrude as a function of the microalgae/total algae ratio, as well as the increased curvature of the figures describing the feedstock composition trends. The promotion of these synergies on the proportions of C, N, O, and HHV of biocrude might be ascribed to the intensification of deoxygenation (decarboxylation, decarbonylation, dehydration), Maillard, Mannich, and amidation reactions, along with the repolymerization of O-rich species for long reaction times. Some of these evolutions are consistent with recent publications (Carpio et al., 2021; Chacón-Parra et al., 2022; Gautam and Vinu, 2020).

3.4.2. Impact of co-HTC temperature and time

Increasing the temperature from 180 to 260 °C augments the proportions of C and H in the biocrude for pure UP and UP-enriched mixtures. However, the proportions of these elements diminish for pure CP and feedstock mixtures with approximately half of CP. Such evolutions result in a similar change in the biocrude HHV. However, the N and O contents in the biocrude produced at 260 °C are higher than those produced at 180 °C regardless of feedstock and processing time. These results are the outcomes of the thermal stability of different components in two kinds of algae and the promotion of deoxygenation reactions at elevated temperatures. On the one hand, macroalgae are abundant in carbohydrates with a low HHV, which are dissolved and depolymerized at a low temperature. Increasing the temperature promotes dehydration, decarbonylation, and decarboxylation reactions, eliminating O from the biocrude (Carpio et al., 2021; He et al., 2020). On the other, the dissolution of energetic lipids, rich in microalgae, occurs at a low temperature, leading to higher C and H proportions and HHV of the biocrude. As the temperature increases, the dissolution and depolymerization of proteins and carbohydrates increase O and N contents in the biocrude, thereby decreasing its HHV. Therefore, the influence of reaction temperature exerts different outcomes for the feedstock mixture containing microalgae and macroalgae.

3.5. Biocrude chemical composition

The biocrude produced from the co-HTC of microalgae and macroalgae contains a pool of chemicals categorized into five groups, with relative chromatographic areas varying depending on the processing conditions. These groups include aliphatic compounds (50–96%), phenols (1–28%), other oxygenated compounds (0–17%), amides (0–23%), and N-heterocycles (1–14%). The detailed chemical composition of the

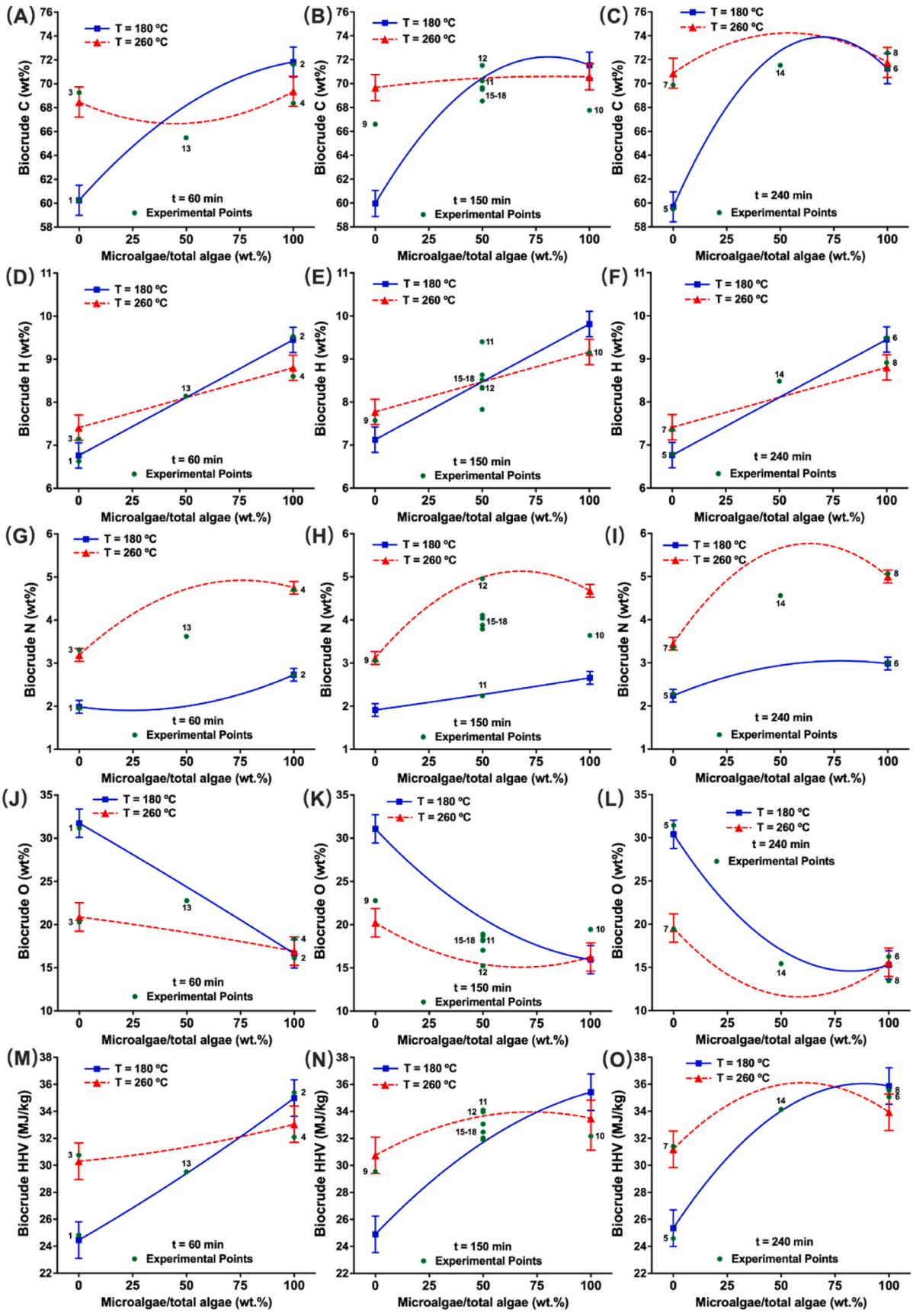

Fig. 4. The Influence of feedstock mix (microalgae and macroalgae) on the elemental composition and HHV of biocrude at 180 and 260 °C for a residence time of 60, 150, and 240 min. Error bars display LSD intervals for the whole variation interval.

biocrude is provided in Table S2. Lipids mainly produce aliphatic compounds, such as hydrocarbons, fatty acids, esters, alcohols, and aldehydes. Phenols are mainly derived from protein degradation, while other oxygenated compounds (aldehydes, furans, alcohols, esters, ketones, and acids) are mainly produced from the degradation and conversion of carbohydrates. Amides arise from the interaction of lipids and protein nitrogen, whereas N-heterocycles (pyridines, pyrroles, indoles, and piperazines) are produced from the interaction of amino acids (degradation from proteins) with lipids and carbohydrates (Gu et al., 2020; Hu et al., 2017; Zhou et al., 2020).

The statistical analyses (Table S1) reveal that the chemical composition of biocrude is primarily influenced by the feedstock composition, which governs the relative contents of aliphatic compounds, phenols, other oxygenated compounds, and N-heterocycles. In parallel, the amide content is primarily influenced by the processing temperature. In addition to these individual effects, the biocrude chemical composition is also affected by the synergies between microalgae and macroalgae. These synergies can be quantified by the contribution of quadratic terms (F^2) relative to the total feedstock influence ($F + F^2$). Such a calculation indicates synergy contributions of 26% for aliphatic compounds, 39% for phenols, 43% for other oxygenated compounds, and 19% for N-heterocycles, while the synergistic effect for amides is insignificant. The impacts of the feedstock mixture on the chemical composition of biocrude are plotted at 200 and 300 °C for 60, 150, and 240 min in Fig. 5.

3.5.1. Influence of the algae feedstock mixture

The impacts of algae feedstock composition on the biocrude composition depend on the co-processing temperature and time. Regardless of co-processing temperature and time, the relative proportion of aliphatic compounds in the biocrude produced from CP is higher than that from UP, while the relative content of N-heterocycles obtained from pure CP is lower. Despite its higher nitrogen fraction, the lower proportion of N-heterocycles in CP biocrude could be ascribed to the dominance of aliphatic compounds masking the relative increment in N-heterocycles content. Transitioning from pure UP to a mixed feedstock leads to a convex increase in the proportion of aliphatic compounds and a concave decrease in N-heterocycle content. The higher proportion of aliphatic compounds can be attributed to the greater lipid content in CP (Table 1) and interactions during co-HTC, such as the disruption of algal cells promoted by acidic species from polysaccharide degradation (Jiang et al., 2018; Zhang et al., 2019; Zhou et al., 2021). Meanwhile, the decrease in N-heterocycles results from their condensation into hydrochar, as evidenced by the increased total nitrogen and pyridinic-N content in hydrochar (Fig. 2 G/H/I and Fig. 3A). These results highlight the synergistic effects between CP and UP in determining biocrude composition. For phenols, other oxygenated compounds, and amides, the effect of feedstock composition varies with the co-processing conditions. At 180 °C, the feedstock mixture does not significantly influence the proportions of phenols and amides. However, increasing macroalgae content leads to a concave decrease in the relative amounts of other oxygenated compounds. This variation possibly arises from the competition of acidic species (e.g., formic acid and acetic acid) that form via polysaccharides depolymerization between polysaccharides and protein degradation. Such a concave drop becomes more marked with prolonged residence time, which could be ascribed to the promotion of the transformation of abundant carbohydrates in macroalgae into organic oxygenated compounds (Jiang et al., 2018; Zhang et al., 2019; Zhou et al., 2021).

At 260 °C, the variation of amides switches into an increased linear pattern. This results from promoting high temperature on the amidation reaction of amino and fatty acids rich in microalgae. Besides, the feedstock composition significantly affects the relative proportion of phenols, which decreases concavely as the proportion of macroalgae in the feedstock increases. Conversely, the feedstock composition has little influence on the relative composition of other oxygenated compounds. These evolutions are accounted for by the repolymerization of such species into hydrochar (as discussed in section 3.4) and the deamination of amino acids to phenols at a high temperature.

3.5.2. Impact of co-HTC temperature and time

Increasing temperature from 180 to 260 °C diminishes the relative composition of aliphatic compounds at the expense of the N-heterocycles content, irrespective of the algal feedstock composition. This arises from converting fatty acids to amides and enhancing Maillard and Mannich reactions involving protein- and carbohydrate-derived compounds at higher temperatures (Chen et al., 2017; Lee et al., 2018; Zhou et al., 2022b). The temperature effect on the relative contents of phenols, other oxygenated compounds, and amides varies depending on the feedstock composition and reaction time. For macroalgae-rich feedstocks, an increment in the temperature diminishes the relative proportion of other oxygenated compounds. On the contrary, such content increases using a feedstock with abundant microalgae. The proportion of phenolic compounds augments with increasing the reaction temperature during the co-HTC of macroalga-enriched mixtures. However, a decrement in phenolic relative content occurs when a microalga-abundant feedstock is used for a reaction time below 150 min.

Prolonging the co-HTT time to 240 min, a higher temperature promotes the formation of phenols regardless of the feedstock composition. As for amides, temperature effects vary with feedstock and reaction time. For UP-rich feedstocks, a rise in the temperature results in a slight decrease in the amides relative content in the biocrude. Conversely, higher temperatures enhance amide formation when co-processing a CP-rich feedstock for a speedy treatment (60 min). After extending the co-processing time above 150 min, the formation of amides is accelerated by augmenting the reaction temperature regardless of the feedstock mixture. These phenomena suggest that higher temperatures promote the deamination of proteins to phenols, the repolymerization of oxygenated compounds from carbohydrates in a macroalgae-rich feedstock, and the amidation of fatty acid and amino acid/ammonia to amides from the microalgae-enriched feedstock (Liu et al., 2021; Zheng et al., 2021; Zhou et al., 2022b). Consequently, processing microalgae-rich feedstocks at high temperatures produces biocrude with high contents of phenols and aliphatic compounds, making it suitable for hydroprocessing into biofuels. For microalgae-abundant feedstocks, increased temperatures produce biocrude rich in amides and N-heterocycles, which could be further separated and purified for N-containing chemical production or subjected to deoxygenation and denitrogenation for biofuel synthesis.

3.6. Distribution of aqueous nitrogen

The concentration of aqueous total nitrogen varies by 519–5375 mg/L, comprising 59–3371 mg/L of organic N, 18–110 mg/L of NO_3^--N, and 279–2462 mg/L of NH_4^+-N. The statistical analyses reveal that the feedstock composition is the primary factor influencing the aqueous nitrogen distribution, whereas the co-processing temperature and time are less influential. As for the synergies, the values of ($F^2/F + F^2$) are 22% for total N, 10% for organic N, 46% for NO_3^--N, and 14% for NH_4^+-N, suggesting substantial synergies between macroalgae and microalgae. Fig. 6A–C/D-F/G-I/J-L plots the influence of feedstock composition on the total N/organic N/NO_3^--N/NH_4^+-N in the aqueous phase at 180 and 260 °C for 60, 150 and 240 min.

3.6.1. Influence of the algae feedstock mixture

The feedstock composition notably impacts the concentrations of total N, organic N, and ammonium N in the aqueous phase. Contrarily, the amount of nitrate N remains at a low level and is primarily governed by processing temperature rather than feedstock composition. The total N, organic N, and NH_4^+-N concentrations increase by augmenting microalgae in the feedstock mixture, regardless of co-processing temperature and time. Most of these variations exhibit non-linear patterns, denoting synergistic/antagonist effects between algal biomasses,

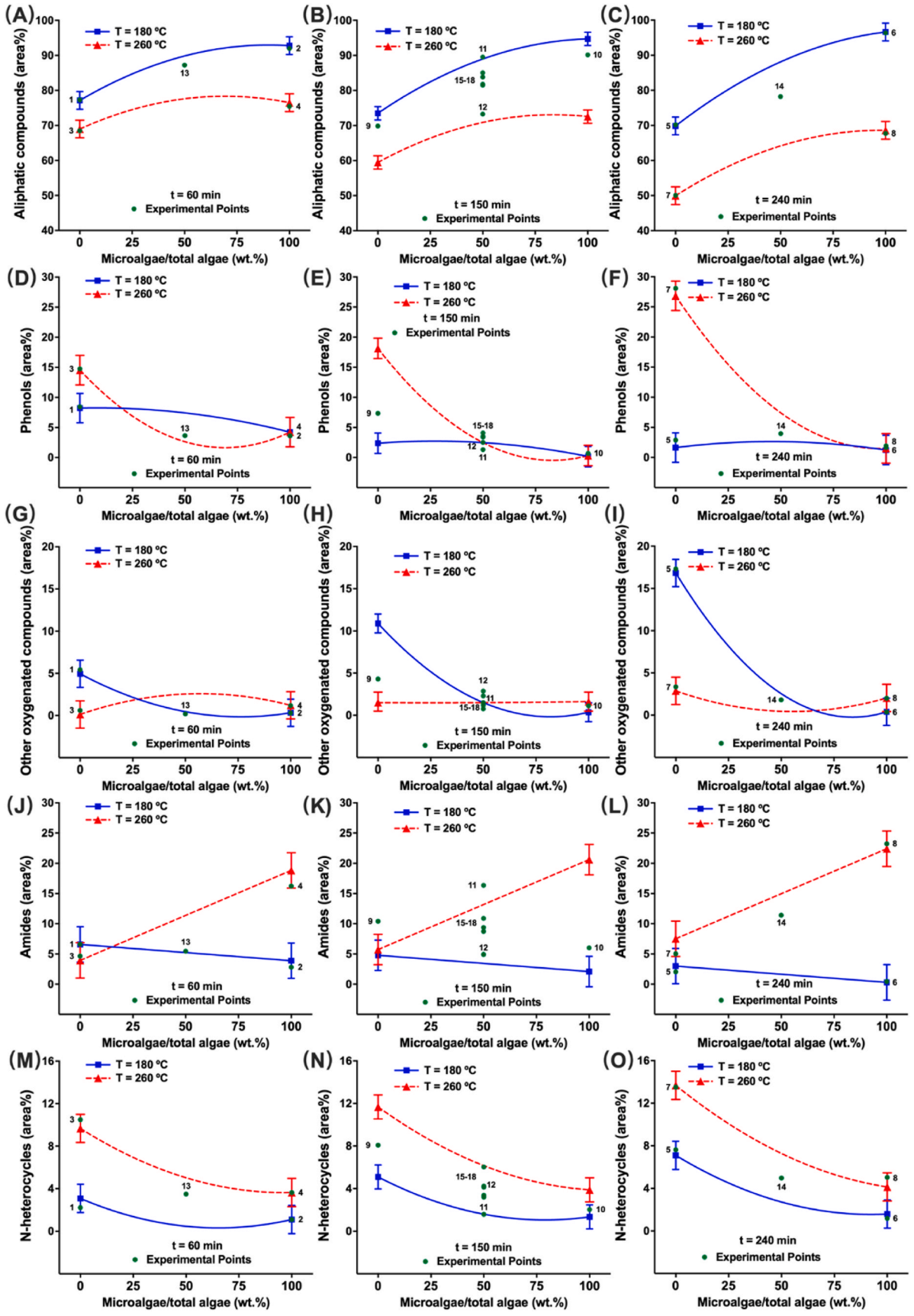

Fig. 5. The Influence of feedstock mix (microalgae and macroalgae) on the chemical composition of biocrude at 180 and 260 °C for a residence time of 60, 150, and 240 min. Error bars display LSD intervals for the whole variation interval.

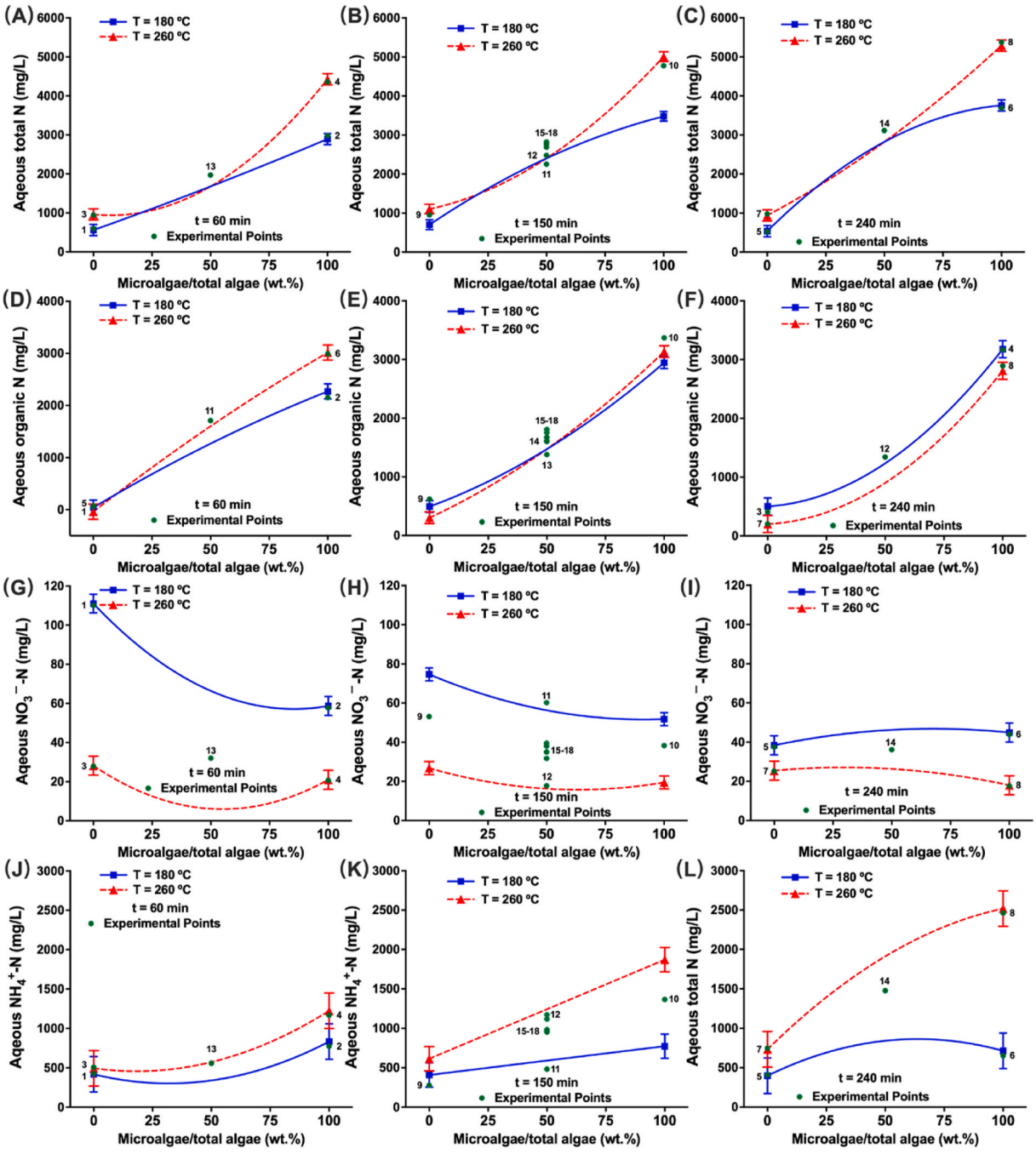

Fig. 6. The Influence of feedstock mix (microalgae and macroalgae) on the aqueous N distribution at 180 and 260 °C for a residence time of 60, 150, and 240 min. Error bars display LSD intervals for the whole variation interval.

directing the distribution of nitrogen species in the aqueous phase. The higher N (protein) content in microalgae accounts for these trends. The protein-N in the feedstock degrades into peptides and amino acids (organic N) and subsequently goes through deamination reactions, forming NH_4^+-N (Yin et al., 2015; Zhuang et al., 2017). The NH_4^+-N could further react with organic acids (abundant in microalgae) to generate amide-N (organic-N) (Jamil et al., 2019). These processes explain the convex evolution of the NH_4^+-N concentration and concave variation in the organic N concentration.

On the contrary, the influence of feedstock composition on the NO_3^--N concentration varies with reaction temperature and time. For a speedy treatment (60 min), augmenting the amount of CP in the feedstock results in a concave diminishment in the NO_3^--N concentration at 180 °C. At 260 °C, the amount of NO_3^--N in the aqueous phase from pure UP is similar to that from pure CP. An initial increase in the microalgae/total algae ratio from 0 to 50 wt% diminishes the NO_3^-N concentration, while a subsequent rise in CP in the feedstock leads to an increment in the NO_3^--N amount. These variations are less critical with prolonged reaction time. This indicates that the degradation of macromolecules in both micro- and macroalgae primarily produces ammonium and organic N in the aqueous phase.

3.6.2. *Impact of co-HTC temperature and time*

The influence of co-processing temperature on the aqueous N distribution depends on the feedstock composition. For a feedstock containing less than 50 wt% microalgae, the impact of co-processing

temperature does not modify the total amount of aqueous N. However, for microalgae-rich feedstocks (more than 50 wt% microalgae), augmenting temperature increases the amount of total aqueous N. This might be accounted for by transferring more nitrogen species in the hydrochar into the aqueous products for a microalgae-rich feedstock, which aligns with the N contents in the hydrochar. As for the organic N, the influence of temperature depends on the residence time. For a speedy co-HTC process (60 min), an increment in the temperature augments the organic N concentration. On the contrary, for a lengthy (240 min) co-HTC process, a temperature increment slightly decreases the organic N amount regardless of the feedstock.

Regarding the inorganic nitrogen species (NO_3^--N and NH_4^+-N), the distribution is significantly influenced by the processing temperature. Increasing the co-processing temperature consistently leads to a rise in NH_4^+-N levels while decreasing NO_3^--N content, irrespective of the feedstock composition. This can be attributed to two key mechanisms: (1) higher temperatures promote the deamination of proteins and amino acids, leading to the accumulation of NH_4^+-N in the aqueous phase, and (2) NO_3^--N undergoes thermal decomposition at elevated temperatures, forming other nitrogenous products, such as gaseous NO_x. These processes collectively explain the observed redistribution of nitrogen species at higher processing temperatures. Prolonging the processing time intensifies the increase in NH_4^+-N but reduces the temperature effect on NO_3^--N. This could be ascribed to the incomplete nitrogen dissolution from the feedstock/hydrochar for a short period and the conversion of organic N to other N species (e.g., ammonia N) for a long processing time.

3.7. Theoretical optimization of the process

Five theoretical optimizations were carried out for the production of N-rich carbonaceous materials (Opt. 1 and 2), solid biofuel (Opt. 3), and both solid and liquid biofuels simultaneously (Opt. 4 and 5). These optimizations were based on the empirical formulae derived from the ANOVA of the experimental data (Table 4). In detail, Optimizations 1 and 2 aim to maximize the production of hydrochar with a high N content and abundant active N-containing functional groups (pyridine and pyrrole-N). Nitrogen doping in carbonaceous materials is known to modify their electronic structure, acidity/basicity, and anchoring sites, resulting in improved performance. Utilizing the nitrogen in algae not only adds value to the hydrochar but also benefits waste management and NO_x emission reduction. Opt. 1 had no feedstock restrictions, whereas Opt. 2 aimed to minimize the microalgae proportion in the feedstock. Optimization 3 intends to produce a solid biofuel with high yield and quality (maximizing the yield and HHV and minimizing the O and N contents). This cleaner solid biofuel offers high energy density and burns with reduced NO_x emissions, supporting sustainable energy applications. Optimizations 4 and 5 aimed to produce energetic solid and liquid biofuels simultaneously. Opt. 4 allowed unrestricted feedstock compositions, while Opt. 5 minimized microalgae usage in the feedstock mixture. This co-production strategy maximizes the utilization of algae feedstocks, enhancing cost and energy efficiency for biorefineries. All the constraints in these optimizations were given relative importance (1 = least important, 5 = most important) to satisfy the intention of the corresponding scenarios. The regression models achieved high coefficients (R^2, $R^2_{adjusted}$, and $R^2_{predicted} > 0.95$), significant signal-to-noise

Table 4
Theoretical optimization: restrictions and optimal conditions.

Optimization	1		2		3		4		5	
	Obj.	Solution	Obj.	Solution	Obj.	Solution	Obj.	Solution	Obj.	Solution
Microalgae/total algae (wt%)		100	−(1)	50		70		100	−(1)	0
Temperature (°C)		260		223		180		260		260
Time (min)		125		174		60		60		240
Global yields										
Hydrochar (%)	+(3)	14.83 ± 0.66	+(3)	22.51 ± 0.66	+(3)	33.87 ± 0.66	+(3)	16.84 ± 0.66	+(3)	19.49 ± 0.66
Biocrude (%)		26.82 ± 0.75		18.77 ± 0.75		6.30 ± 0.75	+(3)	28.53 ± 0.75	+(3)	17.10 ± 0.75
Aqueous + gas (%)		57.40 ± 0.40		58.45 ± 0.40		60.84 ± 0.40		55.78 ± 0.40		63.75 ± 0.40
Hydrochar elemental composition and HHV										
C (wt%)		62.20 ± 1.09		59.18 ± 1.09		59.35 ± 1.09		60.16 ± 1.09		67.63 ± 1.09
H (wt%)		5.99 ± 0.16		5.64 ± 0.16		7.41 ± 0.16		6.27 ± 0.16		5.77 ± 0.16
N (wt%)	+(4)	8.52 ± 0.05	+(4)	5.75 ± 0.05	−(4)	6.75 ± 0.05	−(4)	9.20 ± 0.05	−(4)	3.73 ± 0.05
O (wt%)		22.93 ± 1.08		29.78 ± 1.08	−(4)	26.88 ± 1.08	−(4)	24.63 ± 1.08	−(4)	23.20 ± 1.08
HHV (MJ/kg)		27.28 ± 0.63		24.46 ± 0.63	+(5)	25.66 ± 0.63	+(5)	26.31 ± 0.63	+(5)	28.49 ± 0.63
Hydrochar surface N-species composition										
Pyridine-N (%)	+(5)	19.37 ± 0.93	+(5)	15.50 ± 0.93		11.10 ± 0.93		20.56 ± 0.93		21.34 ± 0.93
Protein-N (%)		61.30 ± 0.54		66.62 ± 0.54		79.18 ± 0.54		64.41 ± 0.54		63.64 ± 0.54
Pyrrole-N (%)	+(5)	9.08 ± 1.16	+(5)	10.09 ± 1.16		2.15 ± 1.16		5.82 ± 1.16		1.48 ± 1.16
Quaternary-N (%)		9.98 ± 0.41		7.76 ± 0.41		5.48 ± 0.41		8.85 ± 0.41		14.71 ± 0.41
Biocrude elemental composition and HHV										
C (wt%)		70.24 ± 0.96		70.11 ± 0.96		70.17 ± 0.96		69.37 ± 0.96		70.87 ± 0.96
H (wt%)		9.14 ± 0.35		8.45 ± 0.35		8.65 ± 0.35		8.80 ± 0.35		7.41 ± 0.35
N (wt%)		4.66 ± 0.13		4.17 ± 0.13		2.21 ± 0.13	−(4)	4.75 ± 0.13	−(4)	3.44 ± 0.13
O (wt%)		16.44 ± 1.54		16.90 ± 1.54		21.28 ± 1.54	−(4)	16.92 ± 1.54	−(4)	19.55 ± 1.54
HHV (MJ/kg)		33.37 ± 1.27		33.37 ± 1.27		31.57 ± 1.27	+(5)	33.05 ± 1.27	+(5)	31.19 ± 1.27
Biocrude chemical composition (area%)										
Aliphatic compounds		73.63 ± 1.81		81.65 ± 1.81		92.21 ± 1.81		76.50 ± 1.81		49.95 ± 1.81
Phenols		0.88 ± 1.56		2.69 ± 1.56		6.42 ± 1.56		4.24 ± 1.56		26.84 ± 1.56
Other oxygenated compounds		1.51 ± 1.03		1.48 ± 1.03		0 ± 1.03		1.21 ± 1.03		2.88 ± 1.03
Amides		20.13 ± 2.41		8.72 ± 2.41		4.68 ± 2.41		18.83 ± 2.41		7.52 ± 2.41
N-heterocycles		3.82 ± 1.10		4.35 ± 1.10		0.33 ± 1.10		3.64 ± 1.10		13.68 ± 1.10
Aqueous N-containing species concentration (mg/L)										
Total N		4880 ± 104		2873 ± 104		2157 ± 104		4426 ± 104		939 ± 104
Organic N		3283 ± 112		1696 ± 112		1700 ± 112		3178 ± 112		202 ± 112
NO_3^--N		19.9 ± 3.1		34.9 ± 3.1		58.9 ± 3.1		21.0 ± 3.1		25.4 ± 3.1
NH_4^+-N		1694 ± 146		1068 ± 146		470 ± 146		1223 ± 146		733 ± 146
Energy efficiency										
E (%)		57.44		65.62		66.20		69.98		69.14

Objectives: + and – represent maximizing and minimizing, respectively. Numbers in brackets are relative optimization importances.

ratios (>4), and insignificant lack-of-fit tests (p-value >0.05) in all models, indicating their reliability and predictive accuracy. Besides, the theoretical results of Opt. 4 and 5 were conducted experimentally (Table S3), which do not show significant differences between them with 95% confidence.

Opt. 1 reveals that a N-rich hydrochar (15% yield) with abundant nitrogen content (8.5 wt%), surface pyridine-N (19%), and pyrrole-N (9%) can be obtained by processing pure microalgae at 260 °C for 125 min. Opt. 2 shows that mixing macroalgae into the feedstock (50 wt %) under the optimum conditions (223 °C, 174 min) increases hydrochar yield (23%) without substantially diminishing N-functional group content (6 wt% N, 16% pyridine-N and 10% pyrrole-N). These optimizations reveal that the synergistic interactions between UP and CP can improve the hydrochar yield and the contents of surface N functional groups, which allows for enhancing N-containing hydrochar production from macroalgae. Regarding solid biofuel, Opt. 3 achieves a high yield (34%) of hydrochar with a high calorific value (26 MJ/kg) from a biomass blend with 70 wt% CP and 30 wt% UP at 180 °C for 60 min. For the coproduction of solid and liquid biofuels, energy-dense hydrochar (17% yield and 26 MJ/kg HHV) and biocrude (28% yield and 33 MJ/kg HHV) are concurrently produced by processing pure CP at 260 °C for 60 min, with a feedstock energy recovery of 70%. This biofuel coproduction can be maintained by processing pure UP at 260 °C for 240 min, with 19% hydrochar (28 MJ/kg) and 17% biocrude (31 MJ/kg) obtained.

The optimization schemes in this work are compared with recent studies, as summarized in Table S4. This study presents various optimization scenarios for the synergistic production of solid biofuels and functional carbonaceous materials. The solid biofuel achieves considerable feedstock energy recovery and a high calorific value of up to 28.5 MJ/kg, comparable to lignite (29 MJ/kg) (Remón et al., 2021). Additionally, the low nitrogen content (below 3.7%) in this solid biofuel, derived from high-nitrogen algae, is exceptional compared to existing studies. This advantage reduces or even eliminates the need for costly post-treatment processes. Moreover, the carbonaceous materials produced exhibit high N retention and abundant N-functional groups, enabling the sustainable production of N-containing carbon directly from biomass feedstocks. This approach eliminates the need for hazardous organic nitrogen sources, contributing to safer and more environmentally friendly practices. Overall, this study provides a more sustainable and efficient breakthrough in utilizing algal feedstocks compared to previous studies (Table 5).

3.8. Nitrogen transformation pathway during co-HTC of microalgae and macroalgae

The potential nitrogen transformation pathways during the co-HTC of microalgae and macroalgae are shown in Fig. 7. At an initial stage, proteins, carbohydrates, and lipids in the feedstock degrade and dissolve into monosaccharides, amino acids and aliphatic compounds (fatty acids, alcohols, and aldehydes). Simultaneously, the degradation of polysaccharides (abundant in macroalgae) generates small organic acids (formic and acetic acids) at low temperatures (Gomes-Dias et al., 2020; Zhang et al., 2019). As for liquid products (biocrude and aqueous fraction), the monosaccharide dehydration forms 5-hydroxymethylfurfural, which is detected in the biocrude produced by UP-rich feedstocks (Table S2). The saccharides and aldehydes react with amino acids via liquid-phase Maillard and Mannich reactions, forming N-heterocycles in the biocrude. Additionally, the cyclization of amino acids also contributes to N-heterocycles formation (Chen et al., 2017; Leng et al., 2023).

For aqueous phase inorganic nitrogen, the deamination of amino acids and proteins generates ammonia-N, accompanied by the formation of phenols and carboxylic acids. The ammonia-N and the amines from amino acid decarboxylation can react with fatty acids via amidation reaction to form amides, contributing up to 23% in the biocrude. As for hydrochar, the carbonization, aromatization, and solid-phase Maillard and Mannich reactions play a dominant role. The N transformation in hydrochar undergoes the following pathways (Lee et al., 2018; Wang et al., 2018): (1) the solid-phase Maillard reaction between the protein-N and carbohydrates to produce pyrrole-N and pyrrole-N; (2) the conversion of pyrrole-N and aldehydes via Mannich reaction to more stable pyridine-N; (3) the cyclization and condensation of the abovementioned N-heterocyclic species to quaternary-N. As temperature increases, these N-containing species on the hydrochar could be further dissolved and liquefied, transferring into the biocrude as N-heterocycles.

The synergies between macroalgae and microalgae feedstocks impact biocrude formation. The acidic species generated from carbohydrate degradation exert an autocatalytic effect on the hydrolysis reactions and, in turn, promote the degradation of polysaccharides and proteins. However, these acidic species are shared between the two degradation reactions, resulting in an antagonist effect on the degradation of carbohydrates to oxygenated compounds. Besides, the positive synergies between protein-rich CP and carbohydrate-rich UP intensify the interactions between proteins and carbohydrate-derived species via Maillard and Mannich reactions. These effects are particularly pronounced at a high temperature (260 °C) for an extended processing time (240 min), accumulating N in the biocrude. However, this synergistic

Table 5
Summary of the HTC of nitrogen-rich biomass from recent publications.

Feedstock	Conditions	Hydrochar yield (%)	HHV (MJ/kg)	N species	ER (%)	Ref.
C. pyrenoidosa	260 °C, 125 min	14.8	27.3	8.5% total N, 19.4% pyridine-N, 9.1%, pyrrole-N	57.4	This work
C. pyrenoidosa and *U. pinnatifida*	70:30 CP: UP, 180 °C, 60 min	33.9	25.7	6.8% total N	66.2	This work
U. pinnatifida	260 °C, 240 min	19.5	28.5	3.7% total N	69.1	This work
C. vulgaris and almond hulls	65:35 C. vulgaris: almond hulls, 200 °C, 20 min	34.2	27.9	4.5% total N	73.6	Zhou et al. (2024)
Cornstalk and *Chlorella*	50:50 cornstalk: Chlorella, 240 °C, 1 h	45	–	3.5% total N, 13% pyridine-N, 27% pyrrole-N	–	Shen et al. (2024)
Microalgae	200 °C, 20 min, 65% seawater	34.2	30.7	4.5% total N	73.6	Zhou et al. (2022b)
Yard waste	220 °C, 6 h	47.1	22.1	9.2% total N	66.5	Venna et al. (2021)
Food waste	220 °C, 6 h	41.5	30.4	10.8% total N	71.2	Venna et al. (2021)
Spirulina	180 °C, 30 min	46	–	9.9% total N, 38% pyridine-N, 10% pyrrole-N	–	Xiao et al. (2019)
Food waste	240 °C, 60 min	38.2	–	3.7% total N, 10.3% pyridine-N, 34.4% pyrrole-N	–	Wang et al. (2018)

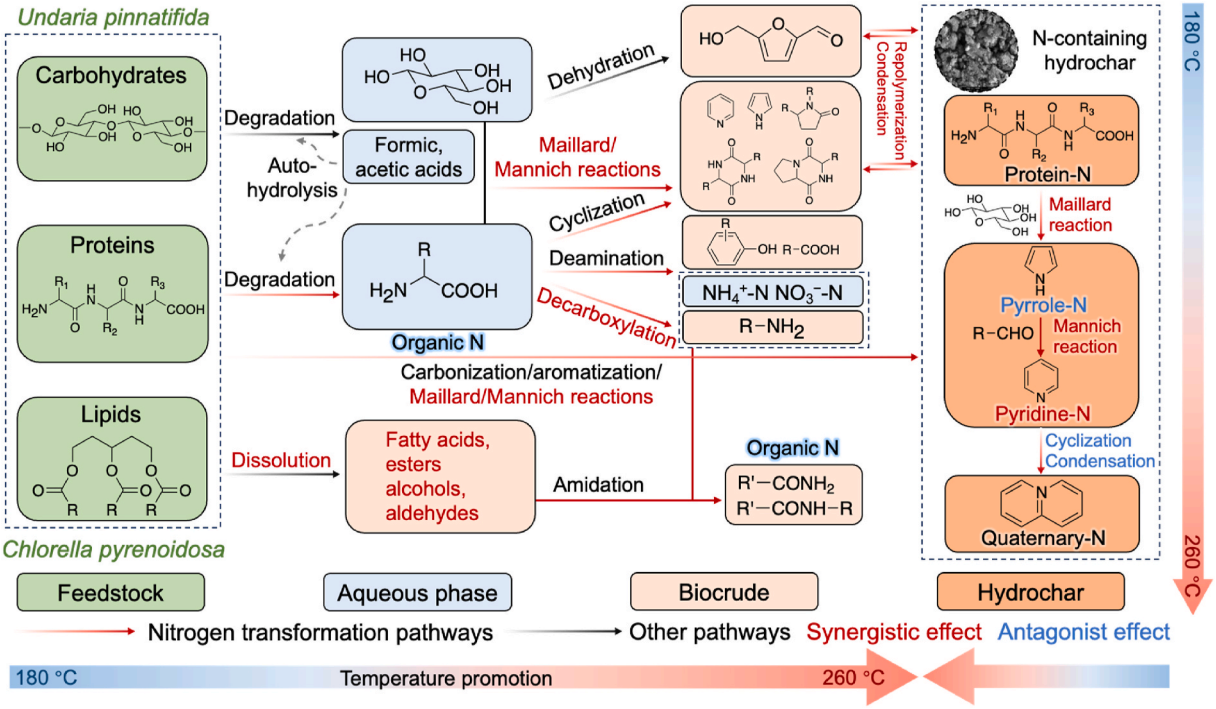

Fig. 7. Nitrogen transformation pathways and synergies during co-HTC of microalgae and macroalgae.

effect does not promote the formation of small-molecule N-heterocycles in the biocrude, possibly due to their condensation into soluble oligomers. Regarding the hydrochar, the synergies between algal biomasses are temperature-dependent. At a low temperature (180 °C), the positive synergies between biomasses promote the formation of hydrochar with a high calorific value, probably ascribed to the enhanced dissolution of O-rich species, deoxygenation reactions of hydrochar and/or the repolymerization of high-HHV components in liquid products. Contrarily, the negative interactions between UP and CP decrease the quality of solid biofuels at a high temperature (260 °C). This might be caused by the interaction between carbohydrates and proteins, which are abundant in macroalgae and microalgae, via solid-phase Maillard and Mannich reactions. These carbohydrate-proteins interactions also increase pyridine-N content while diminishing pyrrole-N content on the hydrochar surface.

4. Conclusions

This study investigated the synergistic co-hydrothermal carbonization (co-HTC) of microalgae (Chlorella pyrenoidosa) and macroalgae (Undaria pinnatifida) under varying temperatures (180–260 °C) and times (60–240 min). The results demonstrate that synergies between microalgae and macroalgae significantly influence product distribution, properties, and nitrogen transformation pathways, with these effects being temperature- and time-dependent. At 180 °C, positive synergies promote high-quality hydrochar production through enhanced deoxygenation reactions and/or repolymerization of energetic liquid components. In contrast, at 260 °C, interactions between carbohydrates and proteins via solid-phase Maillard and Mannich reactions reduce the quality of solid biofuels while enhancing pyridine-N content and decreasing pyrrole-N content on the hydrochar surface. Process optimization revealed that co-HTC can be tailored to produce either N-rich hydrochar or high-calorific-value solid biofuels under different conditions. Specifically, a CP-UP feedstock blend (70:30 wt%) processed at 180 °C for 60 min yields hydrochar with 34% yield and 26 MJ/kg HHV. Incorporating 50 wt% macroalgae into the feedstock increases the hydrochar yield to 23% while maintaining high nitrogen functionality (6 wt% N, 16% pyridine-N, 10% pyrrole-N). Furthermore, the co-production of energy-dense solid and liquid biofuels can achieve up to 70% feedstock energy recovery. These findings provide a foundation for developing efficient, seasonal-free, synergistic algal-based marine biorefineries, advancing nitrogen recycling and sustainable biofuel production. However, challenges remain in scaling up the co-HTC process, particularly with mixed algae feedstocks. Future work should evaluate the economic feasibility of such mixed feedstocks in large-scale applications, including potential challenges such as feedstock sourcing and cost. Additionally, the scalability of co-HTC processes for industrial biorefineries should be thoroughly assessed, considering practical factors like energy efficiency, feedstock cost, and carbon footprint.

Regarding practical applications, nitrogen-rich hydrochar is promising for soil amendment, potentially reducing the need for synthetic fertilizers and enhancing nutrient cycling. The coproduction of biofuels also has significant potential for integration into energy systems, especially in areas seeking sustainable alternatives to conventional energy sources. Specific algae feedstock ratios should be optimized for future research for different applications. For instance, higher nitrogen content in the hydrochar can benefit fertilizer applications, while higher heating value fuels are better suited for energy generation. This study has highlighted the need for further exploration of algae ratios for producing high-nitrogen or high-calorific hydrochars and improving the scalability and cost-effectiveness of co-HTC processes. Exploring the integration of co-HTC into larger, more diverse biorefinery systems will be crucial in realizing the full potential of algal biomass for sustainable biofuel and agricultural applications.

CRediT authorship contribution statement

Yingdong Zhou: Writing – original draft, Methodology, Investigation, Funding acquisition, Formal analysis, Conceptualization. **Haiting Xiao:** Methodology, Investigation, Data curation. **Qing Liu:** Methodology, Formal analysis, Data curation. **Lan Wang:** Methodology, Formal analysis, Data curation. **Yuan Gong:** Methodology, Formal analysis, Data curation. **Javier Remón:** Writing – review & editing, Methodology, Investigation, Conceptualization.

Declaration of competing interest

The authors declare that they have no known competing financial interests or personal relationships that could have appeared to influence the work reported in this paper.

Acknowledgments

This work was funded by the Natural Science Foundation of Sichuan Province (25QNJJ4340) and the Chengdu University of Technology Teachers Development Research Fund (10912-KYQD2022-09753). Javier Remón thanks MCIN/AEI/10.13039/501100011033 and the European Union « NextGenerationEU»/PRTR » for the Ramón y Cajal Fellowship (RYC2021-033368-I) awarded, and the Aragón Government (Research Group Reference T22_23R) for providing frame support.

Appendix A. Supplementary data

Supplementary data to this article can be found online at https://doi.org/10.1016/j.envres.2024.120749.

Data availability

Data will be made available on request.

References

Ayub, H.M.U., et al., 2022. Sustainable valorization of algae biomass via thermochemical processing route: an overview. Bioresour. Technol. 344, 126399.
Benavente, V., et al., 2024. Co-hydrothermal carbonization of microalgae and digested sewage sludge: assessing the impact of mixing ratios on the composition of primary and secondary char. Waste Manag. 174, 429–438.
Boisen, S., et al., 1987. A critical view on the conversion factor 6.25 from total nitrogen to protein. Acta Agric. Scand. 37, 299–304.
Bower, C.E., Holm-Hansen, T., 1980. A salicylate–hypochlorite method for determining ammonia in seawater. Can. J. Fish. Aquat. Sci. 37, 794–798.
Cao, Y., et al., 2021. Hydrothermal carbonization and liquefaction for sustainable production of hydrochar and aromatics. Renew. Sustain. Energy Rev. 152, 111722.
Carpio, R.B., et al., 2021. Effects of reaction temperature and reaction time on the hydrothermal liquefaction of demineralized wastewater algal biomass. Bioresour. Technol. Rep. 14, 100679.
Cataldo, D.A., et al., 1975. Rapid colorimetric determination of nitrate in plant tissue by nitration of salicylic acid. Commun. Soil Sci. Plant Anal. 6, 71–80.
Chacón-Parra, A.D., et al., 2022. Elucidating the maillard reaction mechanism in the hydrothermal liquefaction of binary model compound mixtures and spirulina. ACS Sustain. Chem. Eng. 10, 10989–11003.
Chandrashekhar, V.G., et al., 2022. Nickel-catalyzed hydrogenative coupling of nitriles and amines for general amine synthesis. Science 376, 1433–1441.
Chen, W., et al., 2017. Transformation of nitrogen and evolution of N-containing species during algae pyrolysis. Environ. Sci. Technol. 51, 6570–6579.
Coale, T.H., et al., 2024. Nitrogen-fixing organelle in a marine alga. Science 384, 217–222.
Deng, S., Tabatabai, M., 1994. Colorimetric determination of reducing sugars in soils. Soil Biol. Biochem. 26, 473–477.
Friedl, A., et al., 2005. Prediction of heating values of biomass fuel from elemental composition. Anal. Chim. Acta 544, 191–198.
Gautam, R., Vinu, R., 2020. Reaction engineering and kinetics of algae conversion to biofuels and chemicalsviapyrolysis and hydrothermal liquefaction. React. Chem. Eng. 5, 1320–1373.
Gomes-Dias, J.S., et al., 2020. Valorization of seaweed carbohydrates: autohydrolysis as a selective and sustainable pretreatment. ACS Sustain. Chem. Eng. 8, 17143–17153.
Gu, X., et al., 2020. Recent development of hydrothermal liquefaction for algal biorefinery. Renew. Sustain. Energy Rev. 121, 109707.
Gu, Y., et al., 2022. Co-production of amino acid-rich xylooligosaccharide and single-cell protein from paper mulberry by autohydrolysis and fermentation technologies. Biotechnol Biofuels Bioprod 15, 1.
Hahn, G., et al., 2018. General synthesis of primary amines via reductive amination employing a reusable nickel catalyst. Nat. Catal. 2, 71–77.
Hassan, H., et al., 2024. Unlocking the potential of microalgae: cultivation in algae recycled effluent with domestic wastewater for enhancing biomass, bioenergy production and CO2 sequestration. J. Water Proc. Eng. 68, 106499.
He, S., et al., 2020. Hydrothermal liquefaction of low-lipid algae Nannochloropsis sp. and Sargassum sp.: effect of feedstock composition and temperature. Sci. Total Environ. 712, 135677.
Hu, Y., et al., 2017. Investigation of aqueous phase recycling for improving bio-crude oil yield in hydrothermal liquefaction of algae. Bioresour. Technol. 239, 151–159.
Hu, Y., et al., 2023. Effect of Ni, Mo and W on hydrothermal co-liquefaction of macroalgae and microalgae: impact on bio-crude yield and composition. J. Energy Inst. 110, 101311.
Huang, H.-j., Yuan, X.-z., 2015. Recent progress in the direct liquefaction of typical biomass. Prog. Energy Combust. Sci. 49, 59–80.
Jamil, M.A.R., et al., 2019. Selective transformations of triglycerides into fatty amines, amides, and nitriles by using heterogeneous catalysis. ChemSusChem 12, 3115–3125.
Jana, R., et al., 2025. Boosting of energy efficiency and by-product quality of anaerobic digestion of Kitchen Waste: hybridization with pyrolysis using Zero-Waste strategy. Energy Convers. Manag. 324, 119290.
Jiang, Z., et al., 2018. Mechanistic understanding of salt-assisted autocatalytic hydrolysis of cellulose. Sustain. Energy Fuels 2, 936–940.
Kostyniuk, A., Likozar, B., 2024. Wet torrefaction of biomass waste into value-added liquid product (5-HMF) and high quality solid fuel (hydrochar) in a nitrogen atmosphere. Renew. Energy 226, 120450.
Lee, J., et al., 2018. Hydrothermal carbonization of lipid extracted algae for hydrochar production and feasibility of using hydrochar as a solid fuel. Energy 153, 913–920.
Leng, L., et al., 2021. A review on nitrogen transformation in hydrochar during hydrothermal carbonization of biomass containing nitrogen. Sci. Total Environ. 756, 143679.
Leng, L., et al., 2023. Nitrogen heterocycles in bio-oil produced from hydrothermal liquefaction of biomass: a review. Fuel 335, 126995.
Li, Y., et al., 2019. Correlations between the physicochemical properties of hydrochar and specific components of waste lettuce: influence of moisture, carbohydrates, proteins and lipids. Bioresour. Technol. 272, 482–488.
Lin, H., et al., 2024. Hydrothermal carbonization of pretreated pine needles: the impacts of temperature and atmosphere in pretreatment on structural evolution of hydrochar. J. Anal. Appl. Pyrol. 178, 106421.
Liu, L., et al., 2021. Production of nitrogen-containing compounds via the conversion of natural microalgae from water blooms catalyzed by ZrO2. ChemSusChem 14, 3935–3944.
Manirakiza, P., et al., 2001. Comparative study on total lipid determination using Soxhlet, Roese-Gottlieb, Bligh & Dyer, and modified Bligh & Dyer extraction methods. J. Food Compos. Anal. 14, 93–100.
Matsagar, B.M., et al., 2021. Recent progress in the development of biomass-derived nitrogen-doped porous carbon. J. Mater. Chem. A 9, 3703–3728.
Piccini, M., et al., 2019. A synergistic use of microalgae and macroalgae for heavy metal bioremediation and bioenergy production through hydrothermal liquefaction. Sustain. Energy Fuels 3, 292–301.
Ramachandra, T.V., Hebbale, D., 2020. Bioethanol from macroalgae: prospects and challenges. Renew. Sustain. Energy Rev. 117, 109479.
Remón, J., et al., 2021. Analysis and optimisation of a novel 'almond-refinery' concept: simultaneous production of biofuels and value-added chemicals by hydrothermal treatment of almond hulls. Sci. Total Environ. 765, 142671.
Sahoo, A., et al., 2021. Co-Hydrothermal Liquefaction of algal and lignocellulosic biomass: status and perspectives. Bioresour. Technol. 342, 125948.
Saravanan, A., et al., 2023. Valorization of micro-algae biomass for the development of green biorefinery: perspectives on techno-economic analysis and the way towards sustainability. Chem. Eng. J. 453, 139754.
Sevilla, M., Fuertes, A.B., 2009. The production of carbon materials by hydrothermal carbonization of cellulose. Carbon 47, 2281–2289.
Shen, Q., et al., 2024. Structure evolution characteristic of hydrochar and nitrogen transformation mechanism during co-hydrothermal carbonization process of microalgae and biomass. Energy 295, 131028.
Shen, Y., 2020. A review on hydrothermal carbonization of biomass and plastic wastes to energy products. Biomass Bioenergy 134, 105479.
Shen, Y., et al., 2018. Nitrogen removal and energy recovery from sewage sludge by combined hydrothermal pretreatment and CO2 gasification. ACS Sustain. Chem. Eng. 6, 16629–16636.
Supraja, K.V., et al., 2023. Critical review on production, characterization and applications of microalgal hydrochar: insights on circular bioeconomy through hydrothermal carbonization. Chem. Eng. J. 473, 145059.
Takeyasu, K., et al., 2021. Role of pyridinic nitrogen in the mechanism of the oxygen reduction reaction on carbon electrocatalysts. Angew. Chem. Int. Ed. 60, 5121–5124.
Tian, K., et al., 2020. Single-site pyrrolic-nitrogen-doped sp(2)-hybridized carbon materials and their pseudocapacitance. Nat. Commun. 11, 3884.
Venna, S., et al., 2021. Landfill leachate as an alternative moisture source for hydrothermal carbonization of municipal solid wastes to solid biofuels. Bioresour. Technol. 320, 124410.
Wang, S., et al., 2022a. Study on synergistic mechanism of Co-hydrothermal liquefaction of microalgae and macroalgae. J. Anal. Appl. Pyrol. 164, 105514.
Wang, T., et al., 2018. Influence of temperature on nitrogen fate during hydrothermal carbonization of food waste. Bioresour. Technol. 247, 182–189.
Wang, Z., et al., 2022b. Co-hydrothermal carbonization of sewage sludge and model compounds of food waste: influence of mutual interaction on nitrogen transformation. Sci. Total Environ. 807, 150997.
Xiao, H., et al., 2019. Speciation and transformation of nitrogen for spirulina hydrothermal carbonization. Bioresour. Technol. 286, 121385.
Yin, F., et al., 2015. A detailed kinetic model for the hydrothermal decomposition process of sewage sludge. Bioresour. Technol. 198, 351–357.
Zhang, R., et al., 2019. Selective conversion of hemicellulose in macroalgae enteromorpha prolifera to rhamnose. ACS Omega 4, 7023–7028.
Zheng, Q., et al., 2021. Sulfonated carbon-catalyzed deamination of alanine under hydrothermal conditions. J. Supercrit. Fluids 175, 105275.

Zhou, Y., et al., 2020. Production of high-quality biofuel via ethanol liquefaction of pretreated natural microalgae. Renew. Energy 147, 293–301.
Zhou, Y., et al., 2021. Conversion of polysaccharides in Ulva prolifera to valuable chemicals in the presence of formic acid. J. Appl. Phycol. 33, 101–110.
Zhou, Y., et al., 2022a. Algal biomass valorisation to high-value chemicals and bioproducts: recent advances, opportunities and challenges. Bioresour. Technol. 344, 126371.
Zhou, Y., et al., 2024. An innovative 'sea-thermal' synergetic biorefinery for biofuel production: Co-valorization of lignocellulosic and algal biomasses using seawater under hydrothermal conditions. J. Clean. Prod. 462, 142719.
Zhou, Y., et al., 2022b. Toward developing more sustainable marine biorefineries: a novel 'sea-thermal' process for biofuels production from microalgae. Energy Convers. Manag. 270, 116201.
Zhou, Y., et al., 2023a. Tuning the selectivity of natural oils and fatty acids/esters deoxygenation to biofuels and fatty alcohols: a review. Green Energy Environ. 8, 722–743.
Zhou, Y., et al., 2023b. Hydrothermal conversion of biomass to fuels, chemicals and materials: a review holistically connecting product properties and marketable applications. Sci. Total Environ. 886, 163920.
Zhu, Y., et al., 2024. Predicting the higher heating value of products through solid yield in torrefaction process. Renew. Energy 236, 121446.
Zhuang, X., et al., 2017. The transformation pathways of nitrogen in sewage sludge during hydrothermal treatment. Bioresour. Technol. 245, 463–470.